IEEE Access
Multidisciplinary | Rapid Review | Open Access Journal

Received 21 August 2023, accepted 4 September 2023, date of publication 12 September 2023,
date of current version 21 September 2023.

Digital Object Identifier 10.1109/ACCESS.2023.3314514

RESEARCH ARTICLE

Grey Wolf Optimization Algorithm Based on Follow-Controlled Learning Strategy

HAOJIE ZHANG, JIAXING CHEN, QUNLI ZHANG, ZHIJUN CHEN, XIAOYU DING, AND JIANHUA YAO

College of Mechanical Engineering, Zhejiang University of Technology, Hangzhou 310014, China
Key Laboratory of Special Purpose Equipment and Advanced Processing Technology, Ministry of Education and Zhejiang Province, Zhejiang University of Technology, Hangzhou 310014, China
Institute of Laser Advanced Manufacturing, Zhejiang University of Technology, Hangzhou 310014, China

Corresponding author: Jianhua Yao (lam@zjut.edu.cn)

This research was supported in part by the National Natural Science Foundation of China under Grant 52035014, in part by the Zhejiang Province "Pointer" Research and Development Project (Low Carbon Industry Key Technology and Equipment Research and Development) 2022C03021, and in part by the Zhejiang Province "Pointer" Research and Development Project (Steel Railway Turnout High-energy Bundle Reinforcement Key Technology and Equipment) 2023C01064.

ABSTRACT This paper analyzes the OBL strategy's impact on optimizing the GWO algorithm and identifies three shortcomings. the specific limitations of the OBL optimization approach. To address these three shortcomings and enhance both global optimization and local exploration capabilities of GWO, this paper introduces a follow-controlled opposition learning strategy. then, the paper analyzes the control parameter C of the grey wolf algorithm to investigate its impact on global optimization and local exploration. Based on these properties, a new control parameter C is proposed. The proposed learning strategy and control parameter C are introduced into the traditional grey wolf algorithm to obtain the FCGWO algorithm. Finally, this paper conducts a comparative analysis of the FCGWO algorithm in comparison to other meta-heuristic algorithms, as well as the enhanced grey wolf algorithm, utilizing 23 benchmark test functions and 2 engineering problems. The results indicate that FCGWO effectively avoids the shortcomings of the traditional OBL, while also outperforming other algorithms significantly in terms of solution quality.

INDEX TERMS Meta-heuristic algorithm, grey wolf optimizer, opposition-based learning, optimization.

I. INTRODUCTION

Due to the rapid advancement of science and technology, mathematical optimization problems are increasingly crucial in various engineering fields. To improve processing techniques, it is often necessary to obtain optimal solutions [1] quickly and accurately. Meta-heuristic algorithms, a common approach in global optimization, are employed to tackle various complex problems. In scenarios involving high-dimensional, nonlinear, and non-derivative objective functions, meta-heuristic algorithms often outperform traditional optimization methods [2]. As a result, it is widely used in water engineering [3], [4], power engineering [5], automation technology [6], logistics management [7], and financial engineering [8]. meta-heuristic algorithms are mainly used to simulate the behavior of nature and human beings through mathematical means to achieve optimal solutions. It is divided into four main categories. The first category is evolutionary algorithms that simulate the laws of evolution in nature, mainly Genetic Algorithms (GA) [9], [10], Differential Evolutionary Algorithms (DE) [11], [12]. The second category is group intelligence algorithms that simulate some intelligent behaviors in a group, mainly Particle Swarm Optimization (PSO) [13], [14], and Whale Optimization Algorithm (WOA) [15]. The third category is human behavior algorithms that simulate various behaviors of human individuals or in social groups, mainly Group Search Optimization (GSO) [16], and Social Group Optimization (SGO) [17]. The fourth category is physical algorithms that simulate the existence of objective laws in things in the universe, mainly the Central Force Optimization (CFO) [18], and the Water Wave Optimization (WWO) [19].

The Grey Wolf Optimizer [20] is one of the swarm intelligence optimization algorithms [21], proposed by

The associate editor coordinating the review of this manuscript and approving it for publication was Qiang Li.

Mirjalili et al. from Griffith University, Australia in 2014. This algorithm achieves a globally optimal solution by simulating both the hierarchical structure within a wolf pack [22] and the behaviors involved in tracking, encircling, and attacking prey during hunting [23]. The Grey Wolf Optimization (GWO) has been widely used in the fields of UAV path planning [24], futures price prediction [25], [26], electricity energy optimization [27], [28], predictive optimization of process parameters [29] and supply chain optimization [30], [31], due to its simple structure, less parameter adjustment and high solution accuracy. However, as the complexity of industrial problems increases, GWO faces challenges in continuing to provide effective solutions. The decline in GWO's solution effectiveness primarily arises from the increasing complexity of optimal solution problems. As this complexity grows, so does the prevalence of local optimal solutions. Additionally, the limited population diversity of the grey wolf algorithm poses challenges in achieving a balance between global exploration and local exploration [32], [33], ultimately impacting the algorithm's solution accuracy. Aiming at these problems of the grey wolf algorithm, many scholars have improved the algorithm by enhancing the population diversity and optimizing the control parameters.

Yu et al. [34] proposed the OGWO algorithm by using a nonlinear function to adjust the coefficients while introducing OBL into the GWO algorithm. Singh and Basnal [35] proposed the MDM-GWO algorithm by using mutation-driven as the search mechanism for changing the GWO while optimizing the control parameter a. Millah et al. [36] introduced weighted average, pouncing behavior and nonlinear convergence factor in GWO for traditional OBL optimization and proposed EGWO. Reddy and Narayana et al. [37] proposed a SL-GWO algorithm by introducing symbiotic hunting and learning strategies into GWO in order to avoid falling into local optimal solutions during GWO solving and at the same time to improve solving accuracy. Yuan et al. [38] proposed the elite opposition-based learning strategy (EOBLS), and both introduced EOBLS and chaotic k-best gravitational search strategy (CKGSS) into GWO to obtain the EOCS-GWO algorithm. Long et al. [39] proposed the ROL-GWO algorithm by adding a random number r to the OBL and also proposing a new control parameter C and introducing both into the GWO. Lei et al. [40] proposed the LFGWO algorithm by introducing Lévy flights into GWO in order to avoid premature convergence of the population of GWO and falling into local optimal solutions. Fan et al. [41] used the cosine function to optimize the control parameter a and introduced the beetle antenna strategy and this control parameter into GWO to propose the BGWO algorithm. Long et al. [42] proposed lens backward learning based on lens optical phenomena and improved the control parameter C. Finally, the LIL-GWO algorithm was proposed. Achom et al. [43] improved GWO using fuzzy C means (FCM) and successfully discovered the role played by membrane proteins and viral receptors in the pathogenesis of SARS-CoV-2 infection using this algorithm. Tian et al. [44] proposed a FCM-GWO-BP integrated prediction model for building power consumption using FCM to optimize GWO and found that its RMSPE was reduced by 0.225 compared to BP.

The above-mentioned scholars have effectively improved the solution performance of the GWO algorithm by enhancing population diversity or optimizing control parameters. However, an imbalance issue exists between global search and local exploration. Additionally, researchers did not conduct a thorough analysis of the distribution characteristics of GWO populations during the optimization process. Control parameter optimization primarily focuses on improving the coefficient a with little analysis of the properties and improvements of the control parameter C. To address these problems, this paper proposes a grey wolf optimization algorithm based on follow-controlled learning strategy (FCGWO). The main contributions of this paper are as follows:

(1) Analyzing the distributional properties of oppositional populations in different periods when the GWO of OBL optimization is solving different objective functions reveals the properties exhibited by OBL in solving different functions in different periods.

(2) To enhance both the global optimization and local exploration capabilities of GWO while effectively avoiding the shortcomings of traditional OBL, this paper introduces a Follow-Controlled Learning Strategy.

(3) This paper reveals the impact of different C values on global optimization and local exploration at different stages of the GWO solving process. Simultaneously, a new C control parameter is proposed.

(4) The performance of the FCGWO algorithm proposed in this paper is evaluated on 23 classical test functions and 2 engineering problems. The results demonstrate that FCGWO achieves superior solving efficiency.

II. BASIC ALGORITHM

In this paper, Grey Wolf Optimization algorithms and Opposition-Based Learning strategy are mainly used and their specific mathematical models are described below.

A. GREY WOLF OPTIMIZATION

There is a strict hierarchy within the grey wolf group, which is mainly divided into four classes: α, β, δ, and ω. In the process of rounding up prey, the distance from the prey is used as the evaluation criterion. From near to far, they are α wolves, β wolves, and δ wolves in order, and the rest are ω wolves. The wolves stalk, surround, and attack the prey under the leadership of three head wolves. The specific mathematical model of the GWO is as follows:

Assume that α, β, δ are the optimal, secondary, and third-best points in the preference-seeking process and the other points. Then the mathematical equation for wolf predation on prey is as follows:

1) SURROUNDING THE PREY

$$\mathbf{D} = |\mathbf{C} \cdot \mathbf{X}_P(t) - \mathbf{X}(t)| \tag{1}$$

$$\mathbf{X}(t+1) = \mathbf{X}_p(t) - \mathbf{A} \cdot \mathbf{D} \tag{2}$$

where $\mathbf{X_P}$ represents the location of the prey, t represents the number of iterations, $\mathbf{X}$ represents the current grey wolf location. $\mathbf{A}$ and $\mathbf{C}$ are the coefficient vectors. The expressions are as follows in Eqs. (3) and (4).

$$\mathbf{A} = 2\mathbf{a} \cdot \mathbf{r}_1 - \mathbf{a} \tag{3}$$

$$\mathbf{C} = 2 \cdot \mathbf{r}_2 \tag{4}$$

where $\mathbf{r}_1$ and $\mathbf{r}_2$ are random vectors ranging between [1,0]. $\mathbf{a}$ is a linear convergence factor that decreases linearly from 2 to 0 with the number of iterations t.

2) HUNTING FOR PREY

$$\begin{cases} \mathbf{D}_\alpha = |\mathbf{C}_1 \cdot \mathbf{X}_\alpha - \mathbf{X}| \\ \mathbf{D}_\beta = \left|\mathbf{C}_2 \cdot \mathbf{X}_\beta - \mathbf{X}\right| \\ \mathbf{D}_\delta = |\mathbf{C}_3 \cdot \mathbf{X}_\delta - \mathbf{X}| \end{cases} \tag{5}$$

$$\begin{cases} \mathbf{X}_1 = \mathbf{X}_\alpha - A_1\mathbf{D}_\alpha \\ \mathbf{X}_2 = \mathbf{X}_\beta - A_2\mathbf{D}_\beta \\ \mathbf{X}_3 = \mathbf{X}_\delta - A_3\mathbf{D}_\delta \end{cases} \tag{6}$$

$$\mathbf{X}_{(t+1)} = \frac{\mathbf{X}_1 + \mathbf{X}_2 + \mathbf{X}_3}{3} \tag{7}$$

where $\mathbf{X}_\alpha$, $\mathbf{X}_\beta$ and $\mathbf{X}_\delta$ are the position vectors of α, β, and δ, respectively. $\mathbf{A}_1$, $\mathbf{A}_2$, $\mathbf{A}_3$ and $\mathbf{C}_1$, $\mathbf{C}_2$, $\mathbf{C}_3$ are the control parameters generated by the random vectors $\mathbf{r}$.

3) ATTACKING THE PREY

$$\mathbf{a}(\mathrm{t}) = 2 \times (1 - \frac{t}{Maxlter}) \tag{8}$$

where *Maxlter* is the maximum number of iterations. t is the number of current and iterations. It can be seen that as the number of iterations t increases, a will gradually decrease. At the same time, the value of $|\mathbf{A}|$ also decreases, and when $|\mathbf{A}| < 1$, the wolves start to attack the prey.

B. OPPOSITION-BASED LEARNING

Opposition-Based Learning (OBL) is the mathematical calculation of the current point to generate an opposition point symmetric about the base point. In the global search process of the GWO algorithm, the current point and the opposition point fitness values are calculated and the better point is taken. By this method, the population diversity of GWO is improved to help the algorithm jump out of the local optimal solution. The specific mathematical model of the Opposition-based learning is as follows:

opposition number: If there exists a real number, then its opposition number expression is shown in Eq. (9).

$$x' = a + b - x \tag{9}$$

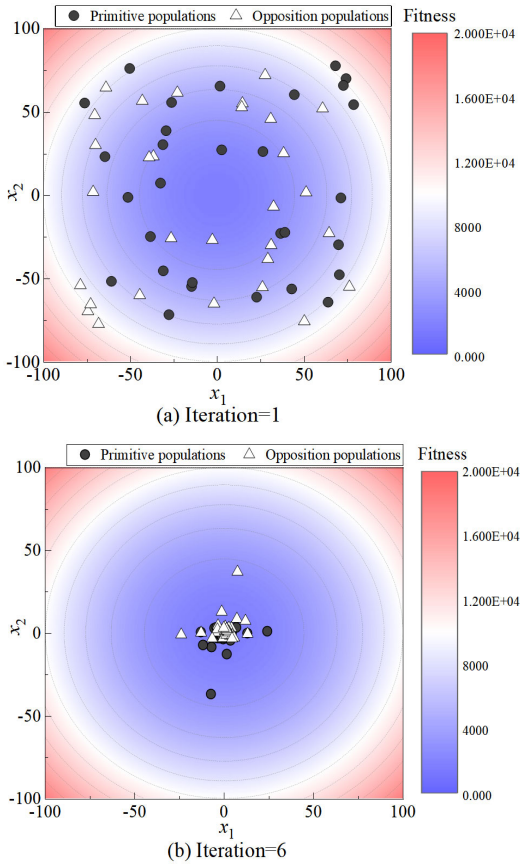

FIGURE 1. Population distribution of OBL-GWO solving Sphere function.

opposition point: Suppose there exists a point $\mathbf{X}$ in the dimensional space and $x_j \in [a, b], j \in (1, 2, 3 \ldots D)$. Thus the opposition point of $\mathbf{X}$ is $\mathbf{X}' = (x'_1, x'_2 \ldots x'_D)$, of which the expression for the members is shown in Eq. (10).

$$x'_j = a_j + b_j - x_j \tag{10}$$

The above opposition number or opposition point about the original point exists in the opposition base point n_j, its expression is shown in Eq. (11).

$$n_j = \frac{a_j + b_j}{2} \tag{11}$$

III. DEFECT ANALYSIS OF OBL IMPROVED GREY WOLF ALGORITHM

The OBL strategy is introduced in the swarm intelligence algorithm mainly to improve the diversity of the population and make the algorithm find a better solution point faster. As a result, numerous scholars have introduced OBL strategies into swarm intelligence algorithms and have effectively improved the algorithm performance. However, many scholars have not made an in-depth analysis of the process of OBL optimization of the swarm intelligence algorithm and the problems involved. For this reason, this section analyzes the optimization process of OBL in the swarm intelligence algorithm before proposing a new backward learning strategy.

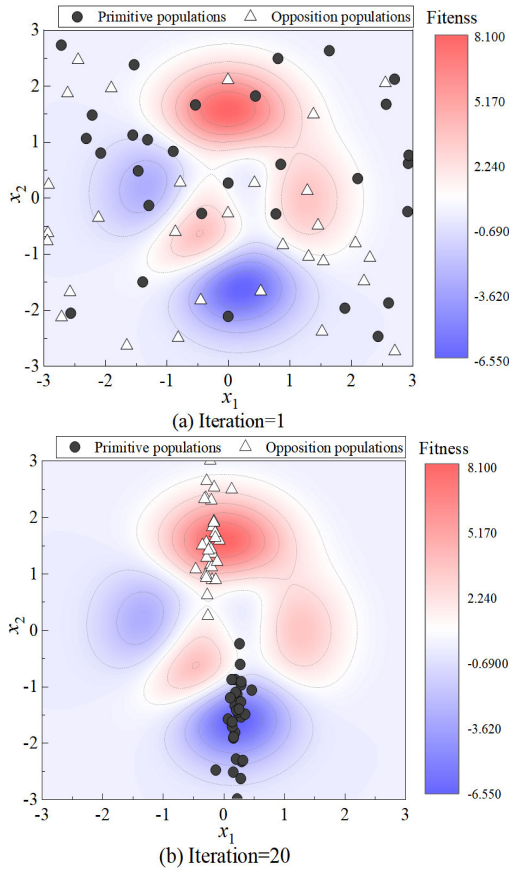

FIGURE 2. Population distribution of OBL-GWO to solve the Peaks function.

A. CONVERGENCE OF OPPOSITION POPULATIONS

The OBL strategy focuses on opposing the current population as a way to generate the opposition population, thus increasing the probability of obtaining the global optimal solution. However, the OBL strategy is effective in increasing population diversity only at the beginning of the iteration. In the middle and late stages, influenced by the distribution of the original population, the opposition population will show significant convergence.

To further illustrate the limitations of the OBL strategy. In this section, the GWO algorithm introducing OBL is used to solve the single-peaked function Sphere. Set the number of populations to 30 and the number of iterations to 500. The number of dimensions is set to 2 for ease of representation. The population distributions for the 1st and 6th iterations of the iterative process are taken and shown in Fig.1

From Fig. 1(a), it can be seen that the introduction of OBL can effectively improve the diversity of the population at the beginning of the algorithm iteration. However, after the original population converges, the opposition population also becomes convergent as shown in Fig. 1(b). When the total number of iterations was 500, the population showed a significant convergence behavior after only 6 iterations. In subsequent iterations, this fast convergence property can

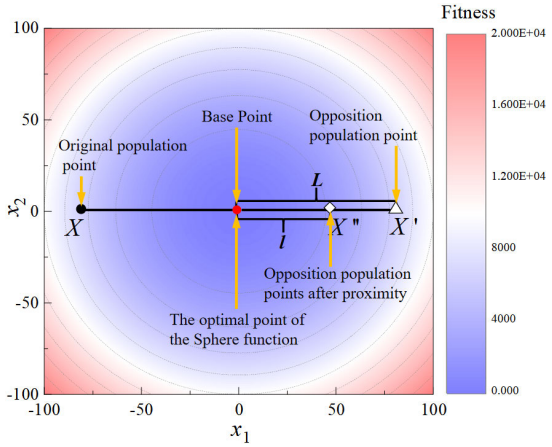

FIGURE 3. Distribution of particularity of OBL solution.

severely limit the effectiveness of OBL in improving population diversity and enhancing the global search for superiority. At the same time, the opposing population and the original population fall in the blue region where the global optimal solution exists as well. This allows us to help improve the accuracy of the local solution in some cases.

In the following, the distribution of opposition populations in OBL-GWO is explored again through the multi-peak function Peaks. The parameter settings are the same as the Sphere function. The population distributions of the 1st and 20th iterations of the iterative process are taken, as shown in Fig. 2.

From Fig. 2(a), it can be seen that at the beginning of the iteration, as with the Sphere function OBL effectively increases the population diversity. However, after 20 iterations, the original population starts to show significant convergence, as shown in Fig. 2(b). At the same time, the opposition populations also inherit the convergence characteristics of the original populations, leading to a limited effect of enhancing diversity. However, the generation position of the opposition population is different in Peaks function than in the Sphere function. As can be seen in Fig. 2(b), the original populations all converge to the blue region where the global optimal solution exists under the GWO, while the opposition populations fall in the red region with the largest fitness value. In this case, the opposing populations not only cannot improve the population diversity but also cannot help to improve the accuracy of the local solution.

B. SPECIFICITY OF OBL OPTIMIZATION SOLUTION

The process of solving the Sphere function for the above OBL-GWO is further analyzed. The opposition base of OBL is found to overlap with the optimal point of the Sphere function. This makes the OBL strategy distinctly specific in optimally solving the optimal points of this class of functions, as shown in Fig. 3.

From Fig. 3, the opposition point generated by Eq. (10) is symmetric about the base point (also the optimal point).

A coefficient r is introduced in Eq. (10).

$$r = \frac{l}{L} < 1 \tag{12}$$

The specific mathematical form of r is not restricted and it is less than 1. Then the OBL expression of the introduced coefficient is shown in (13):

$$x' = a + b - r \cdot x \tag{13}$$

From Fig. 3, it can be observed that the opposition point obtained through Eq. (13) will be closer to the base point (that is also the optimal point). Therefore, it can be concluded that in the case where the optimal point and the base point coincide, introducing a coefficient less than 1 to bring the opposition point closer to the optimal point will result in better optimization performance. In this special case where the opposition base point coincides with the optimal point, the opposition point is always ''pulled'' closer to the optimal solution in each iteration update, and after several iterations, very good optimization results can be obtained. However, when the optimal point does not coincide with the opposition base point, i.e., the optimal point is not at the center of the search space, the optimization effect will be lost. In practical multi-objective optimization problems, it is highly probable that the optimal solution is not located at the center of the search space, and therefore, this special case severely limits the performance of the OBL strategy.

C. FAILURE OF OPPOSITION POPULATIONS IN SYMMETRIC SPACE

Analysis of the mathematical model properties of the Sphere function and OBL reveals that the Opposition-based learning fails when the optimization problem's function is symmetric about the center point of the search space. The proof is as follows:

Suppose there is a function in a two-dimensional space that is symmetric about the n-axis within the interval [a, b] that contains the center axis. Given any point in this interval, its opposition point can be obtained using the opposition learning Eq. (10), as shown in Eq. (14).

$$x' = a + b - r \cdot x \tag{14}$$

As $x = n$ is the central axis, there is Eq. (15).

$$2n = a + b \tag{15}$$

Substituting Eq. (15) into Eq. (14), there is Eq. (16).

$$x_1' = 2n - x_1 \tag{16}$$

Substituting Eq. (16) into the function $f(x)$, there is Eq. (17).

$$f\left(x_1'\right) = f(a + b - x_1) = f(2n - x_1) \tag{17}$$

As $f(x)$ is symmetric about x=n, thus Eq. (18) holds.

$$f\left(x_1\right) = f(2n - x_1) \tag{18}$$

Finally, Eq. (19) is obtained.

$$f\left(x_1'\right) = f(x_1) \tag{19}$$

Generalizing Eq. (19) to n dimensions, there is Eq. (20).

$$f\left(x_1', x_2' \ldots x_n'\right) = f(x_1, x_2 \ldots x_n) \tag{20}$$

Eq. (20) reveals that when the optimization function is symmetric with respect to the center point of the search space, the fitness values of the opposition point and the current point are equal. This property prevents the position of the grey wolf in the original population from being affected by the opposition point, leading to a failure of the Opposition-based learning.

The above analysis indicates that traditional opposition learning strategies encounter several issues when optimizing the GWO algorithm, which can be summarized as follows:

(1) OBL has a limited effect on increasing population diversity: The improvement of population diversity is only effective in the early iterations of the algorithm, and it cannot help the algorithm to improve its solution accuracy in the later stages.

(2) OBL has specificities in optimization problem solving: Introducing a coefficient of less than 1 achieves superior solution effectiveness when the opposition base point overlaps with the optimal point, but it has significant limitations in practical applications.

(3) OBL fails: When the optimization function is symmetric with respect to the center point of the search space, rendering the Opposition-based learning ineffective.

IV. FOLLOW-CONTROLLED OPPOSITION LEARNING STRATEGY

To overcome the limitations of traditional Opposition-Based Learning (OBL) and further improve the solution performance of the Opposition-based learning in the Grey Wolf Optimization algorithm, this paper proposes a Follow-Controlled opposition learning strategy. The strategy mainly consists of two parts, following opposition Learning and population Control Strategy.

A. FOLLOWING OPPOSITION LEARNING STRATEGY

Based on the previous analysis, it is clear that the OBL strategy cannot improve the local exploration ability of GWO in the middle and later stages of iteration, especially for functions whose optimal points are not located at the center of the search space. To overcome this shortcoming, this paper proposes the following mechanism. The core point of this mechanism is to change the upper and lower limit values of OBL in each iteration process, and the specific mathematical description is as follows.

Assuming that the total number of iterations is I, the search space is D dimensional, and the total population size is N, the expression for a certain position point at the i-th iteration is $\mathbf{X}^i = (x_1^i, x_2^i \ldots x_D^i)$ and the total population is $\mathbf{P}^i = (\mathbf{X}_1^i, \mathbf{X}_2^i \ldots \mathbf{X}_N^i)$, where $i \in \{1, 2, \ldots, I\}$. Let $a^i = \max(\mathbf{P}^i)$

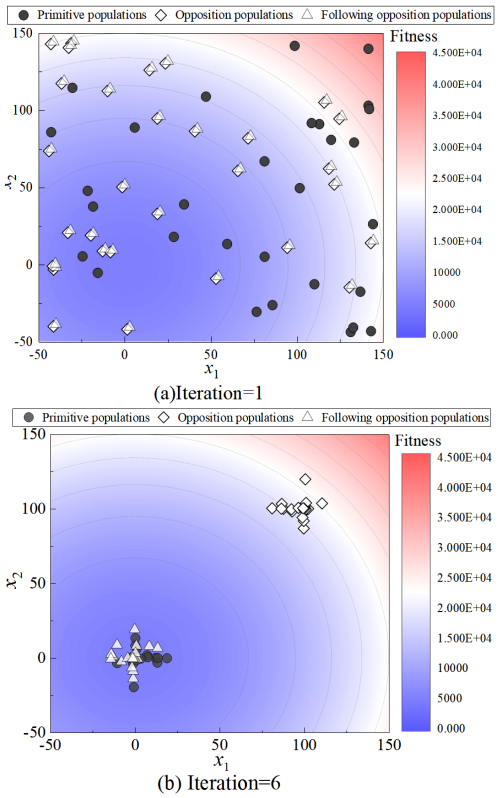

FIGURE 4. Primitive population, opposition population, and following opposition population distribution.

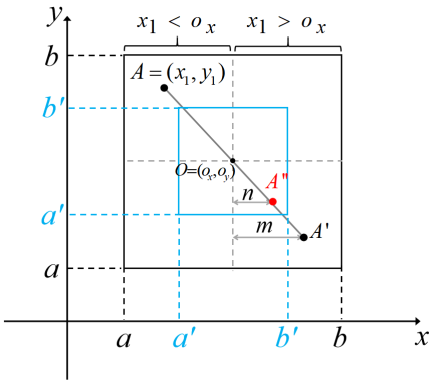

FIGURE 5. Schematic diagram of opposition population controllable relationship.

and $b^i = \min(\mathbf{P}^i)$. Then the following opposition learning strategy is shown in Eq. (21).

$$x^{i\prime} = a^i + b^i - x^i \tag{21}$$

It can be seen from Eq. (21) that after each iteration, the upper and lower limits a^i and b^i, respectively will change to the maximum and minimum dimensional values in the entire population. The introduction of this strategy will cause the opposition reference point to change along with the original population point and also enable the opposition population to free itself from the fixation of the reference point. Therefore, the opposition population can fall into the area being explored by the original population, effectively helping to improve the solution accuracy. The opposition effect is shown in Fig. 4.

The population distribution in Fig. 4 shows that the following opposition learning strategy preserves the enhanced effect of OBL on population diversity, while also extending the solution performance. The specific extensions are as follows:

(1) Fig. 4(a) shows that at *Iter*=1, the population distribution of the following opposition learning strategy is similar to that of the traditional OBL strategy, indicating that the following opposition learning strategy can effectively enhance population diversity in early iterations.

(2) In Fig. 4(b), when the number of iterations is 6, the original population converges to the blue area where the global optimal solution exists under the action of the GWO algorithm. Meanwhile, the following opposition population also ''closely follows'' the original population and falls into the global optimal solution area, indicating that the following opposition population can effectively enhance the local exploration ability of the GWO algorithm.

(3) It can also be observed from Fig. 4(b) that the opposition points generated by the following strategy do not exhibit symmetry about the center point, effectively avoiding the situation where the opposition is ineffective. This indicates that the following opposition population can still effectively enhance the global optimization and local exploration ability of the GWO algorithm in functions that are symmetric about the center point of the optimization space.

B. CONTROLLABILITY OF OPPOSITION POPULATIONS

The proposed opposition learning strategy with a following mechanism mainly addresses the special cases of overlapping between the base point and optimal point and the failure of the opposition population in the original Grey Wolf Optimizer (GWO) algorithm. However, its effectiveness is limited in enhancing global optimization and improving local solution accuracy. To further improve the optimization performance of the GWO algorithm, this paper proposes a controllable opposition population strategy. Its core is to control the size of the opposition population generation area under the following opposition strategy, thus enhancing global optimization ability and improving local solution accuracy. To facilitate the presentation of its changing relationship, a two-dimensional space is used as shown in Fig. 5.

The above Fig.5 shows the upper and lower limits, denoted by a and b, of the original OBL. The upper and lower limits of the OBL that can be controlled through opposition learning of the population are denoted by a' and b'. Point A represents the original point, while A' represents the opposition point, and A'' represents the controllable opposition point. By introducing a scaling factor k, the size of the opposition population generation area can be controlled. The expression for k in Fig. 5 is given by Eq. (22).

$$k = \frac{b' - a'}{b - a} = \frac{n}{m} \tag{22}$$

As point A in 2D satisfies $x_1 < o_x$ and $y_1 > o_y$, under the scaling factor k, the distance to the x-axis and y-axis in each dimension can be expressed as Eq. (23).

$$\begin{cases} o_x - (o_x - x_1) \times k + a \\ o_y + (y_1 - o_y) \times k \end{cases} \tag{23}$$

By opposing the distance relationship in Eq. (23) according to Eq. (10), and opposing the distance relationship of the opposition point under the scaling factor k, Eq. (24) can be obtained.

$$\begin{cases} o_x + (o_x - x_1) \times k \\ o_y \times (y_1 - o_y) - o_y \end{cases} \tag{24}$$

As point O is the center point of the optimization interval, Eq. (25) can be derived.

$$o_y = o_x = \frac{b+a}{2} = \frac{b'+a'}{2} \tag{25}$$

By substituting Eq. (25) into Eq. (24) and simplifying, the opposition relationship of each axis can be obtained, as shown in Eq. (26).

$$\begin{cases} x' = \dfrac{(k+1) \times (a+\mathrm{b})}{2} - k \times x_1 \\ y' = \dfrac{(k+1) \times (a+\mathrm{b})}{2} - k \times y_1 \end{cases} \tag{26}$$

From Eq. (26), it can be seen that regardless of whether the original point is on the left or right side of the base point, *i.e.*, x_1<o_x or x_1>o_x, the same controllable opposition relationship can be obtained. By introducing Eq. (21) into Eq. (26), the final controllable opposition learning expression can be obtained, as shown in Eq. (27).

$$x' = \frac{(k+1) \times (a^i + b^i)}{2} - k \times x \tag{27}$$

In Eq. (27), k is the scaling factor, and by changing its value, the size of the opposition area can be controlled, as shown in Fig. 6.

Fig. 6 shows that the population generated by Eq. (27) not only has an opposite effect but also effectively tracks the range of the original population. When k is 1, only the original population is in opposition. When k is 1.5 and 0.5, the range of the opposition population is enlarged and reduced, respectively, while effectively tracking the distribution area of the original population.

It can be seen that in Eq. (27), k plays an important controlling role in the opposite effect of the population. The selection of the k value has a decisive effect on the optimization effect of the controllable opposition learning in Eq. tracking. The main problem with traditional OBL in the GWO algorithm for optimization is that the convergence speed of the initial population is too fast, and the opposition population in the middle and late stages cannot help improve the solution accuracy. To address this phenomenon, k needs to exhibit an "S" shape with a larger value in the early stage and a smaller value in the later stage. Moreover, it can control the proportion of the "larger value interval" and the "smaller value interval," i.e., the proportion of global search and local exploration. Based

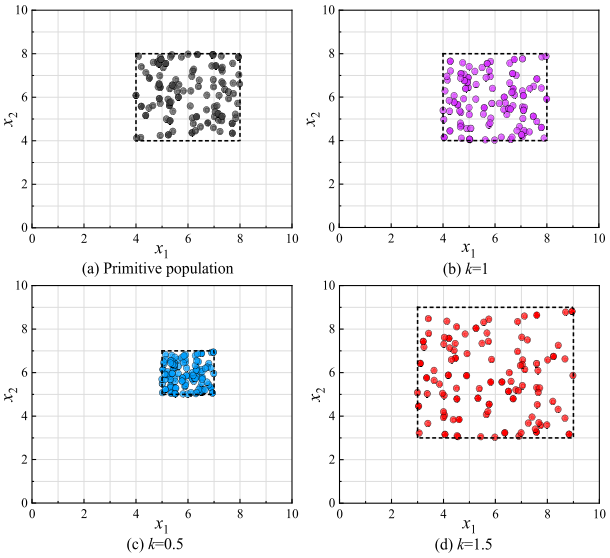

FIGURE 6. Distribution of primitive population and following opposition population.

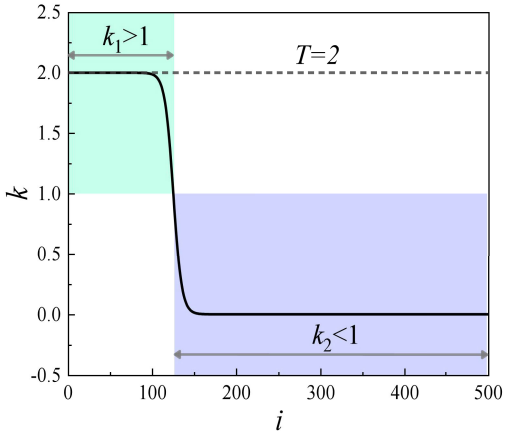

FIGURE 7. Change curve of scaling factor k and iteration number i.

on preliminary experiments and the feature requirements of GWO, the expression of k is determined as Eq. (28).

$$k = \frac{T}{1 + e^{\left[\frac{1}{5} \times (i - \frac{MaxIter}{p})\right]}} = \frac{2}{1 + e^{\left[\frac{1}{5} \times (i - \frac{MaxIter}{4})\right]}} \tag{28}$$

In Eq. (28), i is the current iteration number, *MaxIter* is the maximum number of iterations, T is the maximum control coefficient, and P is the control coefficient for the ratio of global search and local exploration. The distribution of k is shown in Fig. 7.

From Fig. 7, it can be seen that when $i = 0$, k tends to be close to 2 and less than 2, and when $i = 500$, k tends to be close to 0 and greater than 0. The ratio of the number of iterations when $k > 1$ to the number of iterations when $k < 1$ is 1:3, and their sum is the value of p in Eq. (28), which can effectively control the proportion of global optimization and local exploration in the entire solution process. T in Eq. (28) is used to control the initial amplification factor of the

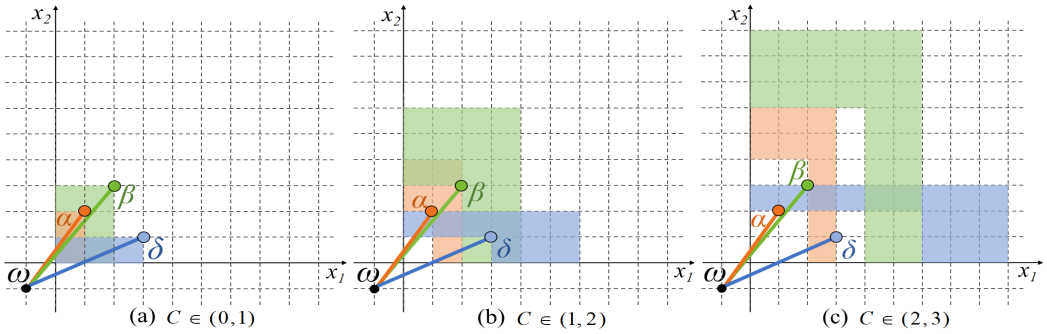

FIGURE 8. Impact of *C* values in different ranges on the range of population migration.

TABLE 1. Effect of control parameter *C* on GWO solution characteristics.

Range	Pre-period (global optimization period)		Mid to late period (Local exploration period)	
$C \leq 2$	Population convergence is fast and consumes fewer iterations.	Poor population diversity makes it easy to fall into local optimal solutions.	The number of iterations for local exploration is high.	The rate of local exploration is slow.
$C > 2$	Strong population diversity and global superiority-seeking ability.	The population convergence is slow and consumes a large number of iterations.	The local solution is faster.	Fewer iterations for a local solution.

population. By changing the values of P and T, the global optimization and local exploration can be effectively adjusted to achieve the optimization of GWO solving performance.

V. ANALYSIS AND IMPROVEMENT OF CONTROL PARAMETER C

A. CHARACTERIZATION OF CONTROL PARAMETER C

This section discusses the exploration and optimization of the solution characteristics of GWO. The previous section introduced a new solution strategy, and this section will focus on the algorithm itself. The main control parameters in GWO are A and C, which have a significant impact on the algorithm's performance. Parameter A controls whether the grey wolves move closer to or farther away from the prey, while parameter C simulates the perception range of different grey wolves in nature. While extensive research has been conducted on parameter A, little is known about parameter C. Therefore, this section will analyze the effect of parameter C on the GWO algorithm's solution characteristics and propose improvement methods based on this effect.

The main objective of improving parameter C in the GWO algorithm is to enhance its global optimization and local exploration capabilities. The former is reflected in the early stages of the algorithm's iterations, where it helps the algorithm locate the region with the optimal solution. The latter is reflected in the later stages of the iteration, where it helps to approximate the optimal value in the optimal solution interval. Parameter C is a random number distributed between 0 and 2, as shown in Eq. (1) and Eq. (4), and its magnitude directly affects the range that each grey wolf can explore. The relationship between the distribution range of C in Eq. (1) and

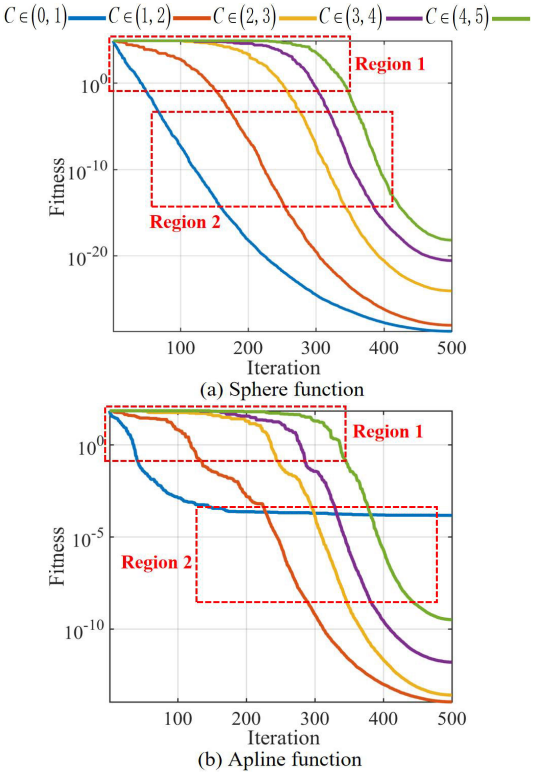

FIGURE 9. Fitness curve of GWO solution function under different *C* value range.

Eq. (4) and its impact is analyzed by plotting, as shown in Fig. 8.

Fig. 8 shows the movable regions of the wolves ω towards the leading wolves α, β, and δ. These regions correspond to

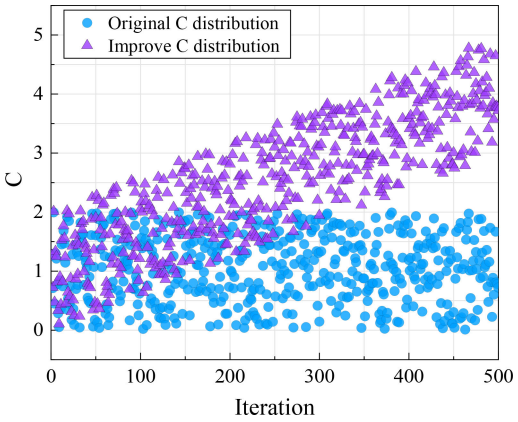

FIGURE 10. Comparison of the distribution of original *C* value and improved *C* value.

the changes in expression (1) under the influence of the control parameter C. The green, orange, and blue regions in the Fig.8 correspond to the possible locations where the wolves ω may stop when moving towards the leading wolves α, β, and δ. As the distribution range of parameter C increases, the wolves take larger steps with larger perception areas. From Fig.8(a) and (b), it can be observed that after each iteration, the wolves ω are distributed on both sides of the prey. However, Fig. 8(c) shows that the wolves ω are at a distance from the prey within the range of $C \in (0,2)$ after each iteration. Although this slows down the speed at which the wolves ω approach the prey, it also widens their roaming range, increases population diversity, and ultimately allows the wolves ω to approach the prey under the influence of control parameter A. The impact of the size of parameter C on population distribution can be summarized as follows: the larger the value of parameter C, the larger the step size of the population's wandering, and the slower the early convergence speed, thus improving the global optimization ability of the algorithm in the early stage.

To further illustrate the specific effects of the control parameter C on the solution process, the fitness curves of GWO with different ranges of C values on the single-peak Sphere function and multi-peak Alpine function are analyzed. To better explore the impact of the C range, the variation interval is set to 1, with the population size and dimension both set to 30 and the optimization range distributed as $[-100,100]$ and $[-10,10]$. The total number of iterations is set to 500, and the results are shown in Fig. 9.

From the changes in the fitness curves in Fig. 9, different ranges of C values have a similar effect on the solution characteristics of single-peak or multi-peak functions. In Region 1 of Fig. 9(a) and (b), it can be observed that as the range of control parameter C increases, the rate of decline in the fitness curve slows down, and the population requires when the value of C is small, the population moves directly when the value of C is small, the population moves directly towards the leading wolf (prey) and converges quickly. However, premature convergence also limits population diversity. In the

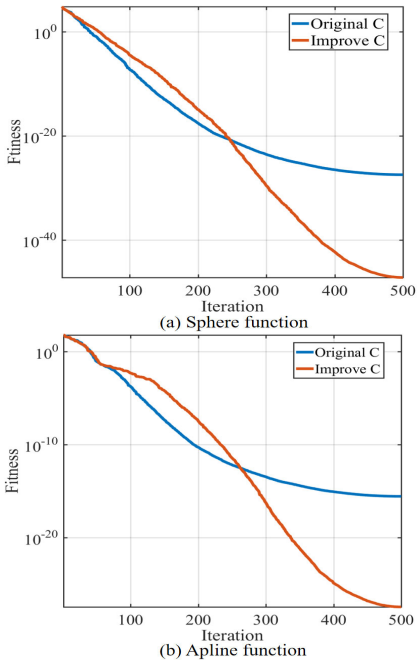

FIGURE 11. GWO solution fitness curve of original *C* value and improved *C* value.

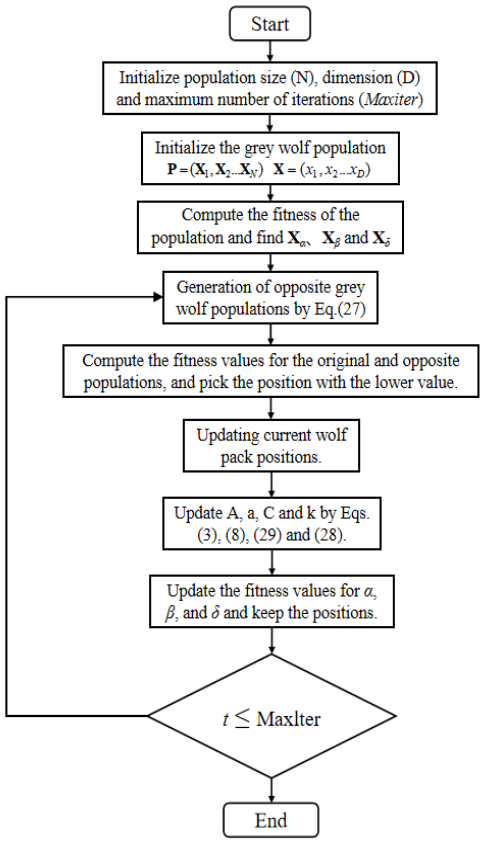

FIGURE 12. Flowchart for building FCGWO.

fitness curve of GWO solving the Alpine function in Region 2 of Fig. 9(b) for $C \in (0,1)$, it can be seen that the algorithm

Name	Expressions	Range	Dim	f_{min}	Type
F1	$f_1(x)=\sum_{i=1}^{n} x_i^2$	[-100,100]	30	0	
F2	$f_2(x)=\sum_{i=1}^{n} \lvert x_i\rvert+\prod_{i=1}^{n} \lvert x_i\rvert$	[-10,10]	30	0	
F3	$f_3(x)=\sum_{i=1}^{n}\left(\sum_{j=1}^{i} x_j\right)^2$	[-100,100]	30	0	
F4	$f_4(x)=\max_i\{\lvert x_i\rvert, 1\le i\le n\}$	[-100,100]	30	0	Unimodal
F5	$f_5(x)=\sum_{i=1}^{n-1}\left[100\left(x_{i+1}-x_i^2\right)^2+\left(x_i-1\right)^2\right]$	[-30,30]	30	0	
F6	$f_6(x)=\sum_{i}^{n}\left(\left[x_i+0.5\right]^2\right)$	[-100,100]	30	0	
F7	$f_7(x)=\sum_{i=1}^{n} ix_i^4+random[0,1)$	[-1.28,-1.28]	30	0	
F8	$f_8(x)=\sum_{i=1}^{n} -x_i\sin\left(\sqrt{\lvert x_i\rvert}\right)$	[-500,500]	30	-418.98*d(dim)	
F9	$f_9(x)=\sum_{i=1}^{n}\left[x_i^2-10\cos(2\pi x_i)+10\right]$	[-5.12,5.12]	30	0	
F10	$f_{10}(x)=-20\exp\left(-0.2\sqrt{\frac{1}{n}\sum_{i=1}^{n} x_i^2}\right)-\exp\left(\frac{1}{n}\sum_{i=1}^{n}\cos(2\pi x_i)\right)+20+e$	[-32,32]	30	0	
F11	$f_{11}(x)=\frac{1}{4000}\sum_{i=1}^{n} x_i^2-\prod_{i=1}^{n}\cos\left(\frac{x_i}{\sqrt{i}}\right)+1$	[-600,600]	30	0	Multimodal
F12	$f_{12}(x)=\frac{\pi}{n}\left\{10\sin(\pi y_1)+\sum_{i=1}^{n-1}(y_i-1)^2\left[1+10\sin^2(\pi y_{i+1})\right]+(y_n-1)^2\right\}+\sum_{i=1}^{n} u(x_i,10,100,4)$	[-50,50]	30	0	
F13	$f_{13}(x)=0.1\left\{\sin^2(3\pi x_1)+\sum_{i=1}^{n}(x_i-1)^2\left[1+\sin^2(3\pi x_i+1)\right]+(x_n-1)^2\left[1+\sin^2(2\pi x_n)\right]\right\}+\sum_{i=1}^{n} u(x_i,5,100,4)$	[-50,50]	30	0	
F14	$f_{14}(x)=\left(\frac{1}{500}+\sum_{j=1}^{25}\frac{1}{j+\sum_{i=1}^{2}\left(x_i-a_{ij}\right)^6}\right)^{-1}$	[-65.536,65.536]	2	1	
F15	$f_{15}(x)=\sum_{i=1}^{11}\left[a_i-\frac{x_1\left(b_i^2+b_i x_2\right)}{b_i^2+b_i x_3+x_4}\right]^2$	[-5,5]	4	0.0003	
F16	$f_{16}(x)=4x_1^2-2.1x_1^4+\frac{1}{3}x_1^6+x_1x_2-4x_2^2+4x_2^4$	[-5,5]	2	-1.0316	
F17	$f_{17}(x)=\left(x_2-\frac{5.1}{4\pi^2}x_1^2+\frac{5}{\pi}x_1-6\right)^2+10\left(1-\frac{1}{8\pi}\right)\cos x_1+10$	[-5,5]	2	0.398	
F18	$f_{18}(x)=\left[1+(x_1+x_2+1)^2\left(19-14x_1+3x_1^2-14x_2+6x_1x_2+3x_2^2\right)\right]\times\left[30+(2x_1-3x_2)^2\times\left(18-32x_1+12x_1^2+48x_2-36x_1x_2+27x_2^2\right)\right]$	[-2,2]	2	3	Fixed dimensional
F19	$f_{19}(x)=-\sum_{i=1}^{4} c_i\exp\left(-\sum_{j=1}^{3} a_{ij}\left(x_j-p_{ij}\right)^2\right)$	[0,1]	3	-3.86	
F20	$f_{20}(x)=-\sum_{i=1}^{4} c_i\exp\left(-\sum_{j=1}^{6} a_{ij}\left(x_j-p_{ij}\right)^2\right)$	[0,1]	6	-3.32	
F21	$f_{21}(x)=-\sum_{i=1}^{5}\left[(X-a_i)(X-a_i)^T+c_i\right]^{-1}$	[0,10]	4	-10.1532	
F22	$f_{22}(x)=-\sum_{i=1}^{7}\left[(X-a_i)(X-a_i)^T+c_i\right]^{-1}$	[0,10]	4	-10.4028	
F23	$f_{23}(x)=-\sum_{i=1}^{10}\left[(X-a_i)(X-a_i)^T+c_i\right]^{-1}$	[0,10]	4	-10.5363	

FIGURE 13. 23 benchmark functions.

falls into a local optimum. In Region 2 of Fig. 9(a) and (b), it is necessary to consume too many iterations when the value of C is large, which is not conducive to improving the accuracy of mid-to-late stage solutions. However, it speeds up the mid-to-late stage solution (solution speed: the degree of fitness value decreases under the same number of iterations). A summary of the impact of different ranges of C values is presented in Table 1 ($C>2$ in the table refers to the relative situation).

B. IMPROVEMENT OF CONTROL PARAMETER C

The paragraph is discussing a new control parameter C proposed in a research paper to improve the performance of GWO in terms of both global optimization ability and local exploration ability. The authors aim to strike a balance between the two aspects. The proposed C value is derived from the original C value range and is modified based on the advantages and disadvantages presented in Table 1. The expression of the new control parameter C is given in Eq. (29).

$$\mathbf{C}=2\times\mathbf{r}_3-3\times\left(\frac{\mathbf{a}}{2}-1\right) \tag{29}$$

where $\vec{r}_3$ is a random vector in the range [1, 0] as $\vec{r}_1$ and $\vec{r}_2$, and a is calculated by Eq. (8). The distribution of C values of Eqs. (4) and (29) are shown in Fig. 10.

In Fig. 10, the improved C also has a variable range of 2 for a single iteration, and it shows a linearly increasing trend overall. It can be observed that the distribution of the improved C is more diverse than the original C, with some increase in the variable range in the early stage, which improves the overall diversity of the population to some extent. Moreover, the distribution of C values in the middle

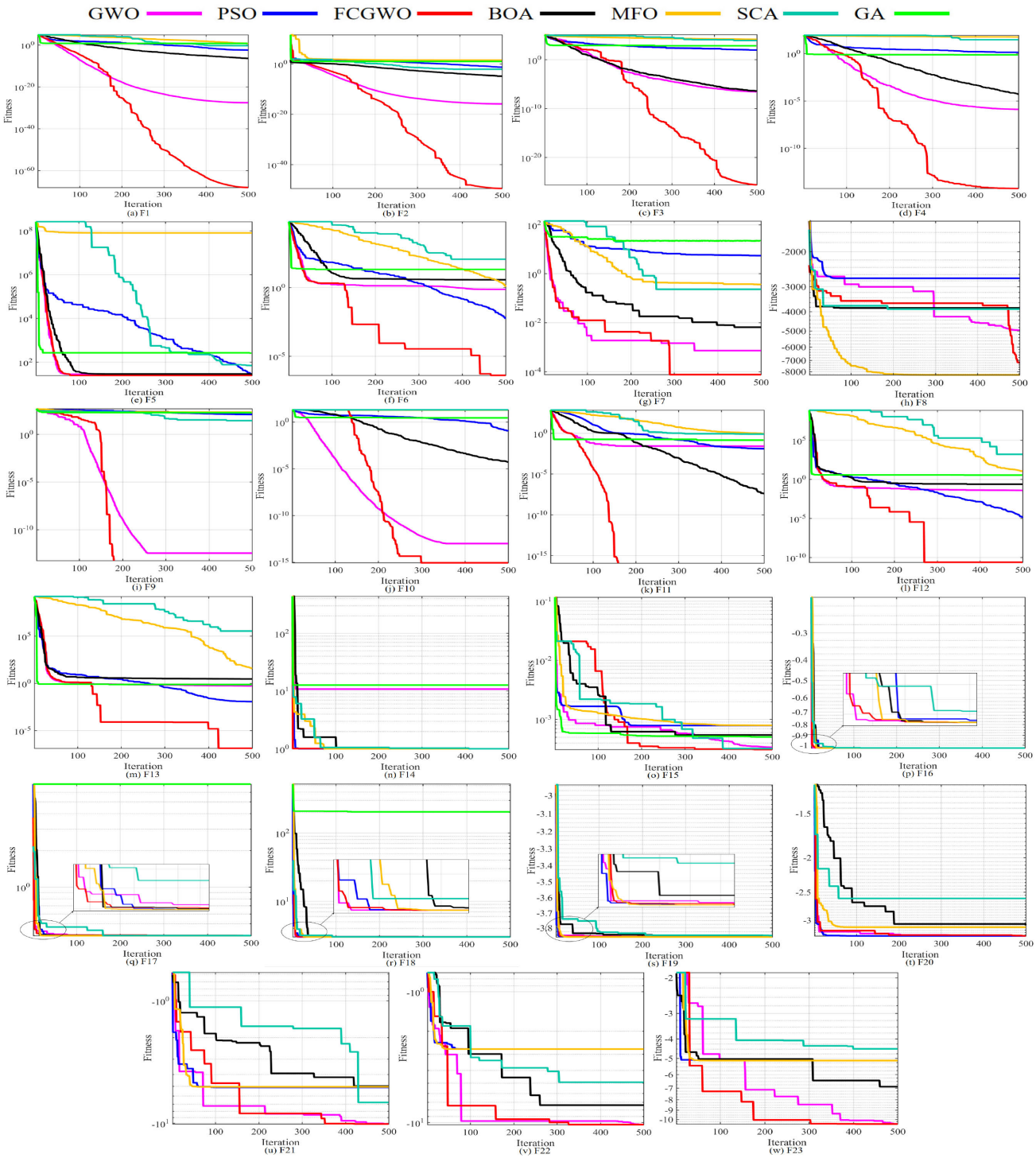

FIGURE 14. Fitness curve of benchmark test function solution.

and later stages is generally larger than that of the original C distribution, which significantly improves the solution speed in the later stages. To validate the performance of the improved C and original C in solving the Sphere and Alpine functions, the same parameters as in Fig. 9 were used, and the results are shown in Fig. 11.

From Fig. 11, it can be seen that the solving curve of the improved C values is weaker than that of the original C values in the early stage. This is because the improved C values increase with the number of iterations in the early stage to enhance the global optimization ability. However, in the middle and later stages, the improved C values significantly

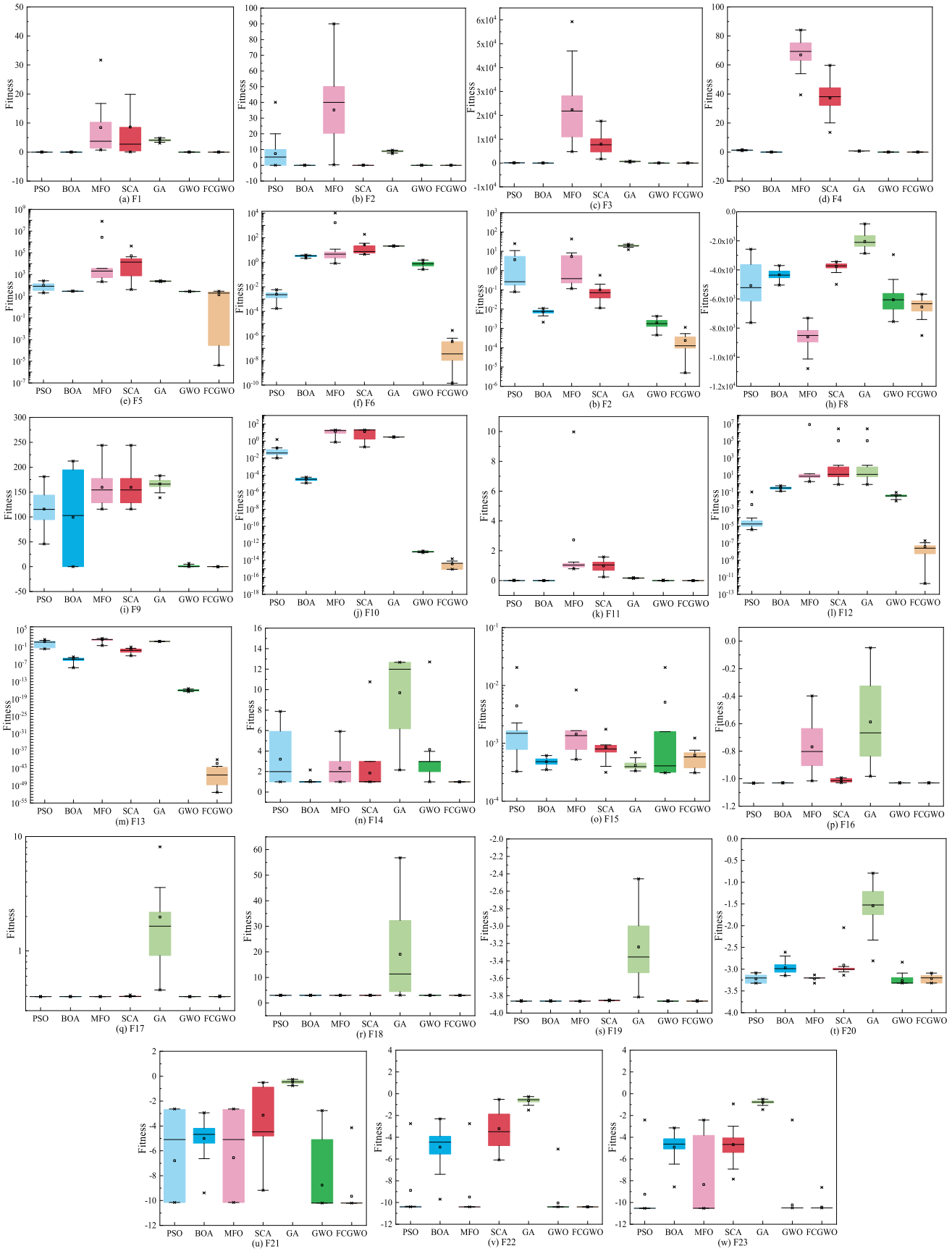

FIGURE 15. Box line diagram of the solution results for the 23 test functions.

outperform the original C values in terms of solution speed. This is because, although the improved C values also increase with the number of iterations, the population has basically converged at this time, and the effect of increasing C is weakened after the control parameter A becomes smaller. Therefore, the increase in C values at this stage only leads to larger steps of the population in the local exploration area than the original C values. This is why larger C values have higher solution speeds in the middle and later stages. The curve changes in Fig. 11 effectively validate the characteristics analysis of C values in Table 1. The construction of FCGWO can be achieved by introducing the above proposed Follow-Controlled Learning Strategy and the control parameter C into the traditional GWO algorithm, and its specific implementation flow is shown in Fig. 12.

VI. EXPERIMENTAL RESULTS AND DISCUSSION

A. BENCHMARK TEST FUNCTION SELECTION

To verify the solving performance of FCGWO algorithm, this study selected 23 common benchmark test functions and conducted simulation calculations to evaluate their solving performance. Among them, F1 to F7 are unimodal test functions; F8 to F13 are multimodal test functions; F14 to F23 are fixed-dimensional multimodal test functions. The specific expressions of each function are shown in Fig. 12

B. COMPARISON WITH OTHER META-HEURISTIC ALGORITHMS FOR SOLVING

To verify the superiority of the FCGWO algorithm, this study compared it with six other swarm intelligence optimization algorithms, including GA [9], [10], PSO [13], [14], GWO [20], BOA [45], MFO [46] and SCA [47]. To increase the validity of the results, each algorithm was run continuously 30 times on the 23 benchmark functions, with the population size set to 30, the maximum iteration number set to 500, and the dimension set according to Fig. 13. Evaluation criteria were based on the average, standard deviation, and best value, and the results are shown in Table 2. To further illustrate the solving performance of FCGWO, an adaptive curve convergence experiment was conducted and compared with the above six algorithms, and the results are shown in Fig. 14. at the same time, a box plot comparison is done for 30 consecutive solutions and the results are shown in Fig. 15.

Table 2 shows that, among the 7 single-peak benchmark functions, except for the Std value of F5, FCGWO performs best in terms of Avg, Std, and Best. Among the 6 multi-peak benchmark functions, FCGWO's Best value is better than that of other optimization algorithms, and it has the best Avg in 4 items and the best Std in 3 items. In the 10 fixed multi-dimensional function solutions, FCGWO also has significant advantages, with the best Avg in 7 items, the best Std in 4 items, and the best in 9 items. The overall statistics of the various optimal solution results in Table 2 are shown in Table 3. It can be seen that FCGWO has Avg, Std, and Best of 19, 12, and 20, respectively, among the 23 tested functions, and all the indexes are shown to be optimal. it can be obviously seen that FCGWO has the best overall solving effect on 23 benchmark functions compared to the other 6 meta-heuristic algorithms.

From the fitness curve in Fig. 14, it can be seen that, except for function F5, FCGWO has a significant advantage in terms of solving speed and accuracy on single-peak functions F1-F7 compared to other algorithms. At the same time, it also has a significant advantage in solving accuracy and speed on multi-peak functions F8-F13.

Where the F8 function is distributed at the boundary due to its optimal point, the spiral search mechanism of MFO can better handle the boundary optimal point problem compared to the center leaning mechanism of GWO. However, MFO's solving effect on other functions is significantly inferior to FCGWO. In the fixed-dimensional function solution, due to the improvement of FCGWO's population diversity, there is no significant advantage in solving speed in the early stage, but its solving accuracy in the later stage is better than that of other algorithms. In addition, compared with the original GWO algorithm, FCGWO has significantly improved its ability in global optimization and local exploration in the 23 benchmark functions. Meanwhile, it can also be seen from the box line diagram of Fig. 15 that among the seven heuristic algorithms for the 23 functions, the overall solution result of FCGWO is the most stable. Among them, the distribution of FCGWO is slightly scattered only on F15 and F20, but it does not have obvious singular values. Overall, FCGWO performs best in the overall solving effect of 23 benchmark functions.

C. COMPARISON WITH OTHER IMPROVED GWO SOLUTIONS

To verify the optimization effect of FCGWO on the above OBL defects, simulations were carried out in the shifted optimization space based on the original optimization space. The shifted optimization space is obtained by offsetting the optimal point on the basis of the original optimization space, so that it is not at the center of the optimization space, but the location of the optimal solution point remains unchanged. This solving space can effectively verify the three OBL defects discovered above: the limited effect of improving population diversity, the limited effect of improving crossover probability, and the opposition failure. To simplify the representation, only 4 functions with the best solutions at [0,0] were selected from the 23 benchmark functions, and the shifted optimization space is shown in Table 4.

In this paper, GWO [20], OGWO [34], ROL-GWO [39] and LIL-GWO [42] algorithms are chosen to do the adaptation curve comparison, and the results are shown in Fig. 16. The following is a line-by-line analysis of the three defects of OBL in combination with the computational results:

(1) Limited effectiveness of OBL in improving population diversity From Fig. 16(c), it can be seen that GWO and OL-GWO are trapped in locally optimal solutions, which is mainly due to the limited population diversity. Although LIL-GWO and ROL-GWO have significant advantages in

TABLE 2. Calculation results of 23 benchmark functions.

Function	Result	PSO	BOA	MFO	SCA	GA	GWO	FCGWO
F1	Avg	2.8977E-03	2.5831E-07	1.6706E+03	1.8277E+01	4.5888E+00	9.1015E-28	**1.3195E-59**
	Std	2.3641E-03	7.5221E-08	3.7896E+03	5.6862E+01	4.0004E-01	1.6711E-27	**7.2272E-59**
	Best	3.4390E-04	1.2485E-07	6.3917E-01	2.2036E-02	3.3714E+00	8.6140E-30	**1.1400E-86**
F2	Avg	4.4146E+00	1.0108E-05	3.6508E+01	2.1882E-02	9.3269E+00	9.9417E-17	**1.5063E-42**
	Std	5.0134E+00	8.8436E-06	2.2982E+01	2.8265E-02	3.6570E-01	7.1497E-17	**6.3453E-42**
	Best	1.3781E-02	6.1312E-08	3.6295E-01	3.5151E-04	8.6167E+00	2.7468E-17	**1.5314E-51**
F3	Avg	9.8757E+01	2.2270E-07	1.9662E+04	8.7194E+03	6.0556E+02	2.2770E-05	**6.2943E-21**
	Std	3.2881E+01	7.6801E-08	1.3506E+04	4.9145E+03	2.0101E+02	7.3138E-05	**3.2951E-20**
	Best	3.6282E+01	7.6341E-08	4.3645E+03	2.2066E+03	2.8261E+02	2.5894E-08	**5.1032E-52**
F4	Avg	1.2575E+00	5.4435E-05	7.0485E+01	3.5110E+01	7.3030E-01	6.9303E-07	**6.2730E-13**
	Std	2.5022E-01	1.0528E-05	9.4519E+00	1.3621E+01	4.4878E-02	6.7974E-07	**2.6369E-12**
	Best	8.4380E-01	3.0322E-05	4.2349E+01	7.8457E+00	5.7276E-01	7.4375E-08	**9.7097E-24**
F5	Avg	1.0368E+02	2.8820E+01	7.4770E+03	4.2037E+04	2.5320E+02	2.6844E+01	**1.0608E+01**
	Std	5.9706E+01	**3.4158E-02**	2.2769E+04	8.1146E+04	1.6130E+01	7.2203E-01	1.2651E+01
	Best	2.1686E+01	2.8751E+01	1.7139E+02	1.4831E+02	2.1373E+02	2.5371E+01	**2.8849E-08**
F6	Avg	2.6380E-03	3.2601E+00	1.6670E+03	1.2779E+01	2.1353E+01	8.1582E-01	**1.5822E-07**
	Std	2.0689E-03	6.1212E-01	3.7822E+03	8.8540E+00	8.8244E-01	4.4496E-01	**2.4323E-07**
	Best	2.1523E-04	1.5322E+00	1.0955E+00	5.0066E+00	1.9187E+01	7.3111E-05	**7.5876E-11**
F7	Avg	4.2691E+00	6.6517E-03	3.4459E+00	1.0013E-01	2.0073E+01	2.0913E-03	**3.2078E-04**
	Std	4.3202E+00	2.6484E-03	7.2203E+00	1.2834E-01	3.6327E+00	9.7922E-04	**3.4590E-04**
	Best	6.7516E-02	9.4216E-04	8.6509E-02	3.8746E-03	9.4487E+00	4.4963E-04	**1.0652E-05**
F8	Avg	-4.7694E+03	-4.3675E+03	**-8.4731E+03**	-3.8150E+03	-2.1552E+03	-5.8122E+03	-7.6243E+03
	Std	1.4483E+03	2.7541E+02	7.7781E+02	**2.6017E+02**	5.4747E+02	1.0196E+03	1.1359E+03
	Best	-6.8245E+03	-4.8709E+03	-1.0058E+04	-4.2467E+03	-3.7640E+03	-7.9059E+03	**-1.0930E+04**
F9	Avg	1.0710E+02	7.1603E+01	1.7198E+02	3.4937E+01	1.7142E+02	2.6132E+00	**0**
	Std	3.2186E+01	9.2582E+01	3.8235E+01	2.7244E+01	8.4081E+00	3.3191E+00	**0**
	Best	4.7354E+01	2.5125E-11	9.5710E+01	6.9262E-02	1.5668E+02	5.6843E-14	**0**
F10	Avg	1.6867E-01	3.1350E-05	1.5879E+01	1.3469E+01	3.0776E+00	9.7167E-14	**1.4803E-15**
	Std	2.9968E-01	1.2541E-05	5.8869E+00	8.9224E+00	8.0398E-02	1.3467E-14	**1.3467E-15**
	Best	2.1303E-02	1.2735E-05	2.3175E+00	3.0328E-01	2.9342E+00	7.5495E-14	**8.8818E-16**
F11	Avg	8.6117E-03	**6.4914E-08**	3.3925E+01	9.6858E-01	1.8825E-01	3.6506E-03	5.9640E-04
	Std	1.0652E-02	**4.6485E-08**	5.5307E+01	4.6923E-01	1.3382E-02	1.0643E-02	3.2666E-03
	Best	4.5893E-05	6.0774E-09	5.4957E-01	2.9117E-01	1.5722E-01	**0**	**0**
F12	Avg	1.7392E-02	3.3813E-01	8.5334E+06	1.9833E+05	3.3845E+00	4.8600E-02	**3.4126E-08**
	Std	3.9257E-02	6.5381E-02	4.6739E+07	1.0691E+06	9.6178E-02	2.7519E-02	**8.0385E-08**
	Best	3.6255E-06	1.7154E-01	1.1176E+00	1.0883E+00	3.1796E+00	1.3084E-02	**4.0238E-13**
F13	Avg	5.1131E-03	2.5800E+00	5.9115E+01	2.4545E+05	6.9302E-01	7.0126E-01	**3.0116E-07**
	Std	6.9480E-03	3.2902E-01	1.8087E+02	8.4993E+05	5.6100E-02	2.9861E-01	**5.0936E-07**
	Best	6.8369E-05	1.9137E+00	1.8559E+00	3.2564E+00	5.2284E-01	1.8986E-01	**7.6340E-11**
F14	Avg	2.9027E+00	1.0320E+00	2.1195E+00	1.9266E+00	1.0743E+01	3.8434E+00	**9.9800E-01**
	Std	2.6223E+00	1.8134E-01	1.5711E+00	1.0043E+00	3.3008E+00	3.6644E+00	**8.9191E-10**
	Best	9.9800E-01	9.9800E-01	9.9800E-01	9.9801E-01	1.6699E+00	9.9800E-01	**9.9800E-01**
F15	Avg	5.5176E-03	**4.5260E-04**	1.6883E-03	1.1380E-03	5.2178E-04	3.7397E-03	8.5204E-04
	Std	8.3374E-03	**1.0082E-04**	3.5519E-03	3.6519E-04	1.4951E-04	7.5635E-03	3.6943E-04
	Best	3.1924E-04	3.2609E-04	4.0754E-04	5.7863E-04	3.2748E-04	3.0769E-04	**3.0810E-04**
F16	Avg	-1.0316E+00	-1.0316E+00	-1.0316E+00	-1.0316E+00	-4.8006E-01	-1.0316E+00	**-1.0316E+00**
	Std	6.5195E-16	7.2432E-05	6.7752E-16	2.6361E-05	2.8903E-01	2.8174E-08	7.5248E-07
	Best	-1.0316E+00	-1.0316E+00	-1.0316E+00	-1.0316E+00	-9.9927E-01	**-1.0316E+00**	**-1.0316E+00**
F17	Avg	3.9789E-01	3.9817E-01	3.9789E-01	4.0003E-01	1.4358E+00	3.9789E-01	**3.9855E-01**
	Std	0.0000E+00	3.5949E-04	**0**	2.3772E-03	1.0562E+00	3.5878E-06	2.2466E-03
	Best	3.9789E-01	3.9789E-01	3.9789E-01	3.9797E-01	4.0369E-01	3.9789E-01	**3.9789E-01**
F18	Avg	5.7000E+00	3.0046E+00	3.0000E+00	3.0001E+00	3.7469E+01	3.0000E+00	**3.0000E+00**
	Std	1.4789E+01	5.8466E-03	**1.6981E-15**	8.1237E-05	3.1650E+01	4.4767E-05	2.8846E-05
	Best	3.0000E+00	3.0000E+00	3.0000E+00	3.0000E+00	3.0068E+00	3.0000E+00	**3.0000E+00**
F19	Avg	-3.8612E+00	-3.8427E+00	-3.8628E+00	-3.8544E+00	-3.2043E+00	-3.8605E+00	**-3.8602E+00**
	Std	3.2065E-03	2.7173E-02	**2.7101E-15**	2.5894E-03	4.3513E-01	2.9291E-03	3.1851E-03
	Best	-3.8628E+00	-3.8624E+00	-3.8628E+00	-3.8622E+00	-3.8425E+00	-3.8628E+00	**-3.8627E+00**
F20	Avg	-3.2036E+00	-2.9475E+00	-3.2150E+00	-2.8912E+00	-1.4896E+00	**-3.2605E+00**	-3.2268E+00
	Std	1.6949E-01	1.3778E-01	8.6151E-02	3.8650E-01	4.2957E-01	8.1349E-02	**7.9510E-02**
	Best	-3.3220E+00	-3.1977E+00	-3.3220E+00	-3.1672E+00	-2.6009E+00	-3.3220E+00	-3.3218E+00
F21	Avg	-7.7240E+00	-4.3388E+00	-7.4809E+00	-2.1011E+00	-5.0472E-01	-9.5658E+00	**-9.7156E+00**
	Std	3.1241E+00	1.2244E+00	3.4080E+00	1.7010E+00	**1.9674E-01**	1.8233E+00	1.6654E+00
	Best	-1.0153E+01	-8.8073E+00	-1.0153E+01	-4.9445E+00	-9.3955E-01	-1.0153E+01	**-1.0153E+01**
F22	Avg	-7.3269E+00	-4.8949E+00	-7.9977E+00	-3.6666E+00	-6.5256E-01	**-1.0401E+01**	-1.0182E+01
	Std	3.4310E+00	1.4489E+00	3.4956E+00	1.4715E+00	2.8819E-01	1.1619E-03	**1.2049E+00**
	Best	-1.0403E+01	-8.6909E+00	-1.0403E+01	-5.4164E+00	-1.6982E+00	-1.0403E+01	**-1.0403E+01**
F23	Avg	-8.4393E+00	-5.4269E+00	-7.3860E+00	-3.8481E+00	-7.9125E-01	-1.0534E+01	**-1.0536E+01**
	Std	3.3021E+00	1.5713E+00	3.5171E+00	1.8297E+00	2.2117E-01	**1.3164E-03**	1.8581E-03
	Best	-1.0536E+01	-1.0205E+01	-1.0536E+01	-7.9379E+00	-1.5054E+00	-1.0536E+01	**-1.0536E+01**

TABLE 3. Statistical table of evaluation indicators for the results of the calculation of the 23 benchmark functions.

Function	Type	Result	PSO	BOA	MFO	SCA	GA	GWO	FCGWO
F1~F7	Uni		0	0	1	0	0	0	6
F8~F13	Mul	avg	0	1	1	0	0	0	4
F14~F23	Fix		0	1	0	0	0	2	7
F1~F7	Uni		0	1	0	0	0	0	6
F8~F13	Mul	Std	0	1	0	1	0	0	4
F14~F23	Fix		1	1	3	0	1	1	3
F1~F7	Uni		0	0	0	0	0	0	7
F8~F13	Mul	Best	0	0	0	0	0	1	6
F14~F23	Fix		0	0	0	0	0	2	8
	Uni	avg	0	1	1	0	0	0	19
Total	Mul	std	1	2	1	1	0	1	12
	Fix	Best	0	2	3	0	1	5	20

TABLE 4. Optimization space area after offset.

Function Name	Original search space	Offset Optimization Space	Optimum point
F1	$[-100,100]^n$	$[-50,150]^n$	$[0,0]^n$
F2	$[-100,100]^n$	$[-50,150]^n$	$[0,0]^n$
F3	$[-5.12,5.12]^n$	$[-2.56,7.68]^n$	$[0,0]^n$
F10	$[-32,32]^n$	$[-16,48]^n$	$[0,0]^n$

solution accuracy compared to FCGWO, as shown in the solution graphs 3-15(g) after offset optimization, their solution effects are significantly inferior to FCGWO. This is because LIL-GWO and ROL-GWO ''pull'' the opposition point closer to the optimal point, leading to particularity in the solution.

(2) Speciality of OBL optimization solution As shown in Fig.s 16(a) and (b), ROL-GWO and LIL-GWO have significant advantages in solution accuracy compared to other algorithms in the original optimization space. This advantage is due to the particularity of the OBL optimization solution, where the original opposition learning base point coincides with the optimal point. In these two algorithms, introducing a scaling factor of less than 1 ''pulls'' all the opposition populations closer to the opposition base point (optimal point), thus significantly improving the solution accuracy. However, in the offset optimization space in Fig.s 16(e) and (f), the non-coincidence of the opposition base point and the optimal point causes a significant decrease in the solution accuracy of ROL-GWO and LIL-GWO, even similar to GWO. At this point, FCGWO has the highest solution accuracy, and the same phenomenon is observed in F9 and F10.

(3) OBL opposition failure. The four functions selected in Fig. 16 are symmetric about the center point of the optimization space. As shown in the fitness curves of the original optimization space for the four functions in Fig. 16(a)-(d), the curve distribution of OL-GWO and GWO overlap almost entirely. The slight differences in curve distribution are caused by the variation of the random number r. This is because the fitness values after the opposition of the functions symmetric about the center are the same, resulting in the population's position being unaffected by the OBL strategy.

The solution results in Fig. 16 validate that FCGWO can effectively overcome the three shortcomings of OBL mentioned above. Although ROL-GWO and LIL-GWO utilize the opposition solving specificity and perform very well in the original optimization space, their effectiveness is limited to the special case where the opposition base point and the optimal point overlap. Once this specificity disappears, their solving efficiency will be significantly reduced. However, in actual engineering optimization problems, the optimal point is unlikely to be at the center point, which makes FCGWO more widely applicable.

D. ENGINEERING PROBLEM SOLVING

1) PRESSURE VESSEL DESIGN

The problem of pressure vessel design [48] is to effectively control the welding and manufacturing cost of the device under the premise of ensuring the safety and reliability of the device. Among them, the cost is mainly controlled by

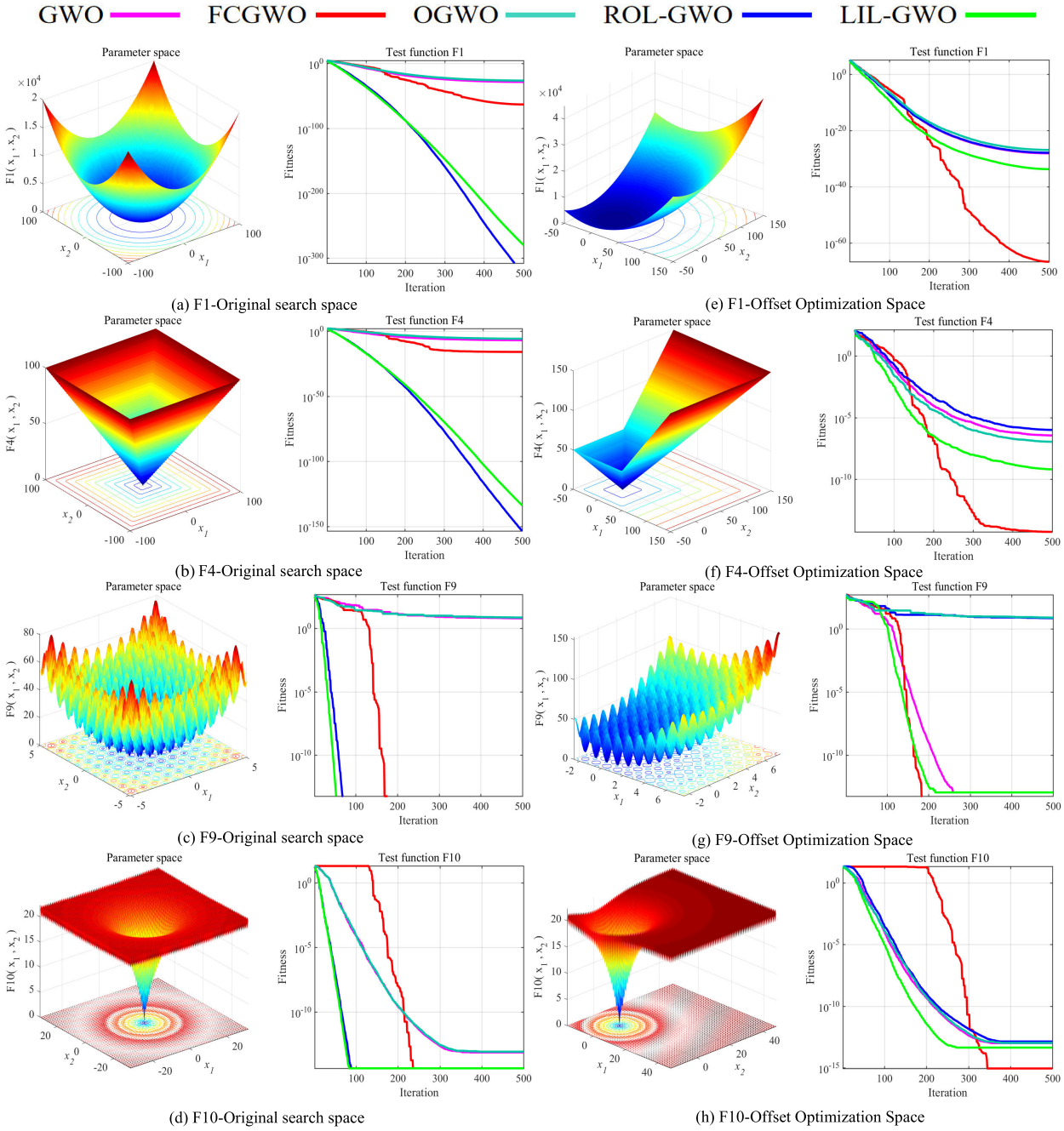

FIGURE 16. Comparison of FCGWO and other opposition strategy GWO solutions.

controlling the head thickness T_h, vessel inner diameter R, cylinder length L, cylinder thickness T_s. The structure is shown in Fig. 17, and the relationship between cost and parameters is as follows:

$$\mathbf{X} = (x_1, x_2, x_3, x_4) = (T_S, T_h, R, L) \tag{30}$$

Minimize:

$$f(x) = 1.7781x_2x_3^2 + 0.6224x_1x_3x_4 + 3.1661x_1^2x_4 + 19.84x_1^2x_3 \tag{31}$$

Subject to:

$$\begin{cases} g_1(x) = 0.00954x_3 - x_2 \le 0 \\ g_2(x) = 0.00193x_3 - x_1 \le 0 \\ g_3(x) = x_4 - 240 \le 0 \end{cases} \tag{32}$$

With bounds:

$$\begin{cases} 10 \le x_3, x_4 \le 200 \\ 1 \le x_2, x_1 \le 99 \end{cases} \tag{33}$$

This paper proposes FCGWO with other 6 meta-heuristic algorithms and 3 improved GWO algorithms to carry out the

TABLE 5. Pressure vessel solution results.

Algorithms	T_S	T_h	R	L	Result
PSO	13.3165	7.1833	42.0822	176.8423	6061.7867
BOA	16.4567	9.1308	47.3753	123.4037	7214.1958
MFO	18.2671	7.7101	48.1418	113.8071	7561.6785
SCA	13.2136	7.5842	40.6804	200.0000	6536.5407
GA	33.5926	58.5227	56.6200	93.6256	34442.1196
GWO	13.7374	6.7484	45.2788	140.8921	6098.4194
OGWO	12.6818	6.6619	42.0765	177.0240	6065.0840
ROL_GWO	14.4269	6.5316	45.3292	140.3351	6091.4962
LIL-GWO	0.7804	0.3900	40.4066	198.8601	5906.4461
FCGWO	0.7782	0.3846	40.3196	200.0000	**5885.3328**

TABLE 6. Reducer solution results.

Algorithms	b	m	p	l_1	l_2	d_1	d_2	Result
PSO	3.5012	0.7000	17.0000	7.7670	8.1924	3.3550	5.2881	3011.5872
BOA	3.6000	0.7000	17.0000	7.3000	8.3000	3.4805	5.5000	3222.5427
MFO	3.6000	0.7000	28.0000	7.3000	8.3000	3.4674	5.4938	5728.2494
SCA	3.6000	0.7000	17.0000	8.3000	8.3000	3.3963	5.3946	3137.6700
GA	3.3963	0.6044	21.8069	7.7139	8.0257	3.4614	5.4600	3393.6363
GWO	3.5044	0.7000	17.0024	7.7403	7.9394	3.3704	5.2875	3011.0327
OGWO	3.5004	0.7000	17.0000	7.3379	8.0356	3.3725	5.2905	3010.0375
ROL_GWO	3.5007	0.7000	17.0000	7.5005	7.9370	3.3514	5.2923	3005.1385
LIL-GWO	3.5006	0.7000	17.0000	7.6842	7.7893	3.3592	5.2868	3002.0068
FCGWO	3.5000	0.7000	17.0000	7.3000	7.7153	3.3505	5.2867	2994.4245

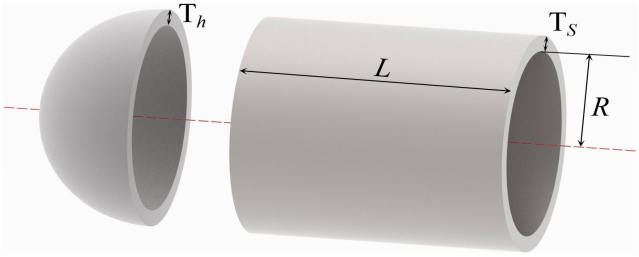

FIGURE 17. Pressure vessel schematic.

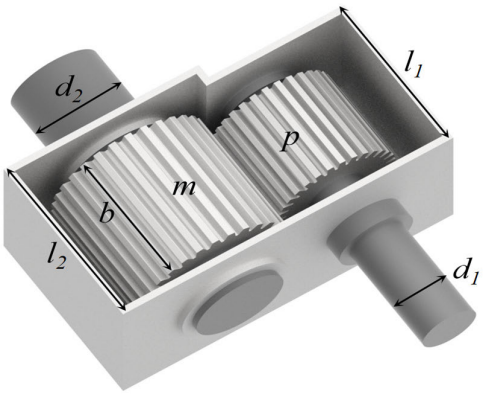

FIGURE 18. Reducer schematic.

speed reducer minimum weight problem solving, the results are shown in Table 5. It can be seen that in the 10 optimization algorithms, FCGWO solution results in the smallest value of only 5885.3328. The structural parameters obtained by the FCGWO. The minimum manufacturing cost of the pressure vessel can be achieved. This effectively shows that FCGWO is significantly better than the other meta-heuristic algorithms in Table 5 in solving the pressure vessel problem.

2) WEIGHT MINIMIZATION OF A SPEED REDUCER

The main objective of the gearbox design problem [49] is to reduce the weight of the gearbox to a minimum while

TABLE 7. Glossary of abbreviations.

Nomenclature	Abbreviation
Grey wolf optimization algorithm based on follow-controlled learning strategy	FCGWO
Genetic Algorithms	GA
Differential Evolutionary Algorithms	DE
Particle Swarm Optimization	PSO
Whale Optimization Algorithm	WOA
Group Search Optimization	GSO
Social Group Optimization	SGO
Central Force Optimization	CFO
Grey Wolf Optimization	GWO
Unmanned Aerial Vehicle	UAV
Opposition-based learning grey wolf optimizer for global optimization	OGWO
Mutation-driven grey wolf optimizer with modified search mechanism	MDM-GWO
Enhanced grey wolf optimization	EGWO
Symbiotic learning-based Grey Wolf Optimizer	SL-GWO
Elite opposition-based learning strategy	EOBLS
Chaotic k-best gravitational search strategy	CKGSS
Elite opposition-based learning and chaotic k-best gravitational search strategy based grey wolf optimizer algorithm	EOCSGWO
A random opposition-based learning grey wolf optimizer	ROL-GWO
Grey Wolf Optimizer With Levy Flight	LFGWO
Lévy fligt	LF
Opposition-Based Learning	OBL
Beetle antenna strategy based grey wolf optimization	BGWO
Grey wolf optimization algorithm based on lens imaging learning strategy	LIL-GWO
Fuzzy C Means	FCM
Back Propagation Neural Network	BP
Sine Cosine Algorithm	SCA
Moth-flame Optimization Algorithm	MFO
Butterfly Optimization Algorithm	BOA

satisfying the bending stresses of the gears, the surface pressure, the transverse deflection of the shafts, and the stresses on the shafts. There are seven variables involved in this problem, the main ones are tooth face width b, tooth module m, number of teeth p, first bearing distance l_1, second bearing distance l_2, first shaft diameter d_1, second shaft diameter d_2, the reducer structure is shown schematically in Fig. 18. The mathematical model is as follows:

$$\mathbf{X} = (x_1, x_2, x_3, x_4, x_5, x_6, x_7) = (b, m_h, p, l_1, l_2, d_1, d_2) \tag{34}$$

Minimize:

$$\begin{aligned} f(x) = {} & 0.7854x_1x_2^2(14.9334x_3 - 43.0934 + 3.3333x_3^2) \\ & + 0.7854(x_5x_7^2 + x_4x_6^2) - 1.508x_1(x_7^2 + x_6^2) \\ & + 7.477(x_7^3 + x_6^3) \end{aligned} \tag{35}$$

Subject to:

$$\begin{cases} g_1(x) = 27 - x_1x_2^2x_3 \le 0 \\ g_2(x) = 397.5 - x_1x_2^2x_3^2 \le 0 \\ g_3(x) = 1.93 - x_2x_3x_4^{-3}x_6^4 \le 0 \\ g_4(x) = 1.93 - x_2x_3x_5^{-3}x_7^4 \le 0 \\ g_5(x) = 10x_6^{-3}\sqrt{16.91 \times 10^6 + (745x_2^{-1}x_3^{-1}x_4)^2} - 1100 \le 0 \\ g_6(x) = 10x_7^{-3}\sqrt{157.5 \times 10^6 + (745x_2^{-1}x_3^{-1}x_5)^2} - 850 \le 0 \\ g_7(x) = x_2x_3 - 40 \le 0 \\ g_8(x) = 5 - x_1x_2^{-1} \le 0 \\ g_9(x) = x_1x_2^{-1} - 12 \le 0 \\ g_{10}(x) = 1.5x_6 - x_4 + 1.9 \le 0 \\ g_{11}(x) = 1.1x_7 - x_5 + 1.9 \le 0 \end{cases} \tag{36}$$

With bounds:

$$\begin{cases} 2.6 \le x_1 \le 3.6 \\ 0.7 \le x_2 \le 0.8 \\ 17 \le x_3 \le 28 \\ 7.3 \le x_4, x_5 \le 8.3 \\ 2.9 \le x_6 \le 3.9 \\ 5 \le x_7 \le 5.5 \end{cases} \tag{37}$$

The weight problem of the gearbox design was addressed using the FCGWO algorithm along with nine other meta-heuristic algorithms, and the results are presented in Table 6. As observed in Table 6, FCGWO produces the best result value. This indicates that with the parameters b=3.5, m = 0.7, p = 17, l_1 =7.3, l_2 =7.7153, d_1 =3.3505, and d_2 =5.2867, it not only meets the speed reducer constraint but also accomplishes lightweight manufacturing effectively. These results highlight the superior performance of FCGWO in addressing gearbox weight design compared to the other meta-heuristic algorithms listed in Table 6.

VII. CONCLUSION

In this study, we analyze the population distribution characteristics of OBL in GWO and elaborate on its defects under various functions and at different stages. To address these defects and enhance the solution performance of GWO, we propose the follow-controlled learning strategy and a new control parameter C. Finally, we compare the proposed FCGWO algorithm with other algorithms using 23 test functions and 2 types of engineering problems. The results demonstrate that FCGWO exhibits superior solution stability and accuracy. The conclusions of this paper can be divided into the following 3 points:

(1) Through analyzing the optimization process of OBL in GWO, three defects were found: (*i*) the Opposition-based learning enhances the limited diversity of the population, which mainly occurs in the later stages where the opposition population inherits the convergence characteristics of the original population, greatly reducing the exploration area, and the convergence of the opposition population cannot help with local exploration; (*ii*) there are special optimization solutions, which mainly exist when the opposition base point coincides with the optimal point. After introducing a coefficient less than 1, the opposition point is "pulled closer" to the optimal point, which can achieve very good solving results, but the applicability is extremely limited; (*iii*) the opposition fails, which mainly occurs when the optimization space is symmetrical about the center point, that is, the fitness values before and after the opposition are the same, which will not affect the position change of the population.

(2) In response to the three defects in OBL optimization in GWO, the FCGWO algorithm is proposed, which mainly changes the upper and lower limits of the original OBL and takes the maximum and minimum values in the entire dimension during each iteration. At the same time, a scaling factor k is introduced in this strategy to control the size of the distribution area of the opposition population during each iteration. Then, the control parameter C of GWO itself was studied, and the influence of different C distribution sizes on solving performance was summarized. Based on this influence characteristic, a new control parameter C was proposed.

(3) FCGWO will be proposed along with six other optimization algorithms for comparison of Avg, Std, and Best results as well as solving fitness curve comparisons in 23 classical benchmark test functions. It is found that FCGWO has a significantly better solving effect than the other six algorithms. Furthermore, the original search space is shifted, and fitness curve comparisons are conducted again with other improved GWO algorithms. It is found that FCGWO effectively overcomes three OBL defects and has a wider range of applications.

This paper provides a detailed elaboration on the population distribution within the GWO solving process, its impact on the solving outcome, and methods to adjust the control strategy, resulting in effective enhancements to the traditional GWO algorithm. According to the excellent solution performance of FCGWO, we can apply it to more engineering problems in the future, such as Prediction of CO storage performance [50] in energy management, hyper-parameter optimization [51] in circuit fault detection, state-of-charge (SOC) estimation [52] in automotive batteries, riverbed load prediction [53] in water conservancy engineering.

APPENDIX

See Table 7.

REFERENCES

[1] K. Wang, M. Guo, C. Dai, and Z. Li, "Information-decision searching algorithm: Theory and applications for solving engineering optimization problems," *Inf. Sci.*, vol. 607, pp. 1465–1531, Aug. 2022.

[2] L. Wang, Q. Cao, Z. Zhang, S. Mirjalili, and W. Zhao, "Artificial rabbits optimization: A new bio-inspired meta-heuristic algorithm for solving engineering optimization problems," *Eng. Appl. Artif. Intell.*, vol. 114, Sep. 2022, Art. no. 105082.

[3] Z. Yang, Y. Wang, and K. Yang, "The stochastic decision making framework for long-term multi-objective energy-water supply-ecology operation in parallel reservoirs system under uncertainties," *Expert Syst. Appl.*, vol. 187, Jan. 2022, Art. no. 115907.

[4] Y. Nishi, H. Koga, and Y. H. Wee, "Multi-objective optimization of an axial flow hydraulic turbine with a collection device to be installed in an open channel," *Renew. Energy*, vol. 209, pp. 644–660, Jun. 2023.

[5] W. Dong, Q. Yang, X. Fang, and W. Ruan, "Adaptive optimal fuzzy logic based energy management in multi-energy microgrid considering operational uncertainties," *Appl. Soft Comput.*, vol. 98, Jan. 2021, Art. no. 106882.

[6] B. Sahu, P. K. Das, and M. R. Kabat, "Multi-robot co-operation for stick carrying application using hybridization of meta-heuristic algorithm," *Math. Comput. Simul.*, vol. 195, pp. 197–226, May 2022.

[7] E. S. Döngül, E. Artantaş, and M. B. Öztürk, "Multi-echelon and multi-period supply chain management network design considering different importance for customers management using a novel meta-heuristic algorithm," *Int. J. Inf. Manage. Data Insights*, vol. 2, no. 2, Nov. 2022, Art. no. 100132.

[8] H.-O. Bae, S.-Y. Ha, M. Kang, H. Lim, C. Min, and J. Yoo, "A constrained consensus based optimization algorithm and its application to finance," *Appl. Math. Comput.*, vol. 416, Mar. 2022, Art. no. 126726.

[9] N. Chen, N. Xie, and Y. Wang, "An elite genetic algorithm for flexible job shop scheduling problem with extracted grey processing time," *Appl. Soft Comput.*, vol. 131, Dec. 2022, Art. no. 109783.

[10] N. Shah, H. El-Ocla, and P. Shah, "Adaptive routing protocol in mobile ad-hoc networks using genetic algorithm," *IEEE Access*, vol. 10, pp. 132949–132964, 2022.

[11] R. Storn and K. Price, "Differential evolution—A simple and efficient heuristic for global optimization over continuous spaces," *J. Global. Optim.*, vol. 11, no. 4, pp. 341–359, Dec. 1997.

[12] J.-Y. Li, Z.-H. Zhan, K. C. Tan, and J. Zhang, "A meta-knowledge transfer-based differential evolution for multitask optimization," *IEEE Trans. Evol. Comput.*, vol. 26, no. 4, pp. 719–734, Aug. 2022.

[13] S. Molaei, H. Moazen, S. Najjar-Ghabel, and L. Farzinvash, "Particle swarm optimization with an enhanced learning strategy and crossover operator," *Knowl.-Based Syst.*, vol. 215, Mar. 2021, Art. no. 106768.

[14] H. Pang, W. Fan, F. Liu, L. Duan, S. Liu, J. Wang, and W. Quan, "Design of highly uniform field coils based on the magnetic field coupling model and improved PSO algorithm in atomic sensors," *IEEE Trans. Instrum. Meas.*, vol. 71, pp. 1–11, 2022.

[15] S. Mirjalili and A. Lewis, "The whale optimization algorithm," *Adv. Eng. Softw.*, vol. 95, pp. 51–67, May 2016.

[16] B. Wu, C. H. Qian, and W. H Ni, "The improvement of glowworm swarm optimization for continuous optimization problems," *Expert. Syst. Appl.*, vol. 39, no. 7, pp. 6335–6442, Jun. 2012.

[17] S. Satapathy and A. Naik, "Social group optimization (SGO): A new population evolutionary optimization technique," *Complex Intell. Syst.*, vol. 2, no. 3, pp. 173–203, Aug. 2016.

[18] Y. Liu and P. Tian, "A multi-start central force optimization for global optimization," *Appl. Soft Comput.*, vol. 27, pp. 92–98, Feb. 2015.

[19] Y.-J. Zheng, "Water wave optimization: A new nature-inspired metaheuristic," *Comput. Oper. Res.*, vol. 55, pp. 1–11, Mar. 2015.

[20] S. Mirjalili, S. M. Mirjalili, and A. Lewis, "Grey wolf optimizer," *Adv. Eng. Softw.*, vol. 69, pp. 46–61, Mar. 2014.

[21] J. Krause, G. D. Ruxton, and S. Krause, "Swarm intelligence in animals and humans," *Trends Ecol. Evol.*, vol. 25, no. 1, pp. 28–34, Jan. 2010.

[22] L. D. Mech, "Alpha status, dominance, and division of labor in wolf packs," *Can. J. Zool.*, vol. 77, no. 8, pp. 1196–1203, Nov. 1999.

[23] C. Muro, R. Escobedo, L. Spector, and R. P. Coppinger, "Wolf-pack (Canis lupus) hunting strategies emerge from simple rules in computational simulations," *Behavioural Processes*, vol. 88, no. 3, pp. 192–197, Nov. 2011.

[24] C. Qu, W. Gai, J. Zhang, and M. Zhong, "A novel hybrid grey wolf optimizer algorithm for unmanned aerial vehicle (UAV) path planning," *Knowl.-Based Syst.*, vol. 194, Apr. 2020, Art. no. 105530.

[25] J. Liang and G. Jia, "China futures price forecasting based on online search and information transfer," *Data Sci. Manage.*, vol. 5, no. 4, pp. 187–198, Dec. 2022.

[26] X. Wang, X. Li, and S. Li, "Point and interval forecasting system for crude oil price based on complete ensemble extreme-point symmetric mode decomposition with adaptive noise and intelligent optimization algorithm," *Appl. Energy*, vol. 328, Dec. 2022, Art. no. 120194.

[27] A. Naserbegi and M. Aghaie, "Exergy optimization of nuclear-solar dual proposed power plant based on GWO algorithm," *Prog. Nucl. Energy*, vol. 140, Oct. 2021, Art. no. 103925.

[28] M. Ghalambaz, R. J. Yengejeh, and A. H. Davami, "Building energy optimization using grey wolf optimizer (GWO)," *Case Stud. Thermal Eng.*, vol. 27, Oct. 2021, Art. no. 101250.

[29] T. Adithiyaa, D. Chandramohan, and T. Sathish, "Optimal prediction of process parameters by GWO-KNN in stirring-squeeze casting of AA2219 reinforced metal matrix composites," *Mater. Today, Proc.*, vol. 21, pp. 1000–1007, Jan. 2020.

[30] A. M. Fathollahi-Fard, M. A. Dulebenets, M. Hajiaghaei–Keshteli, R. Tavakkoli-Moghaddam, M. Safaeian, and H. Mirzahosseinian, "Two hybrid meta-heuristic algorithms for a dual-channel closed-loop supply chain network design problem in the tire industry under uncertainty," *Adv. Eng. Informat.*, vol. 50, Oct. 2021, Art. no. 101418.

[31] B. Mosallanezhad, M. A. Arjomandi, O. Hashemi-Amiri, F. Gholian-Jouybari, M. Dibaj, M. Akrami, and M. Hajiaghaei-Keshteli, "Metaheuristic optimizers to solve multi-echelon sustainable fresh seafood supply chain network design problem: A case of shrimp products," *Alexandria Eng. J.*, vol. 68, pp. 491–515, Apr. 2023.

[32] Q. M. Alzubi, M. Anbar, Y. Sanjalawe, M. A. Al-Betar, and R. Abdullah, "Intrusion detection system based on hybridizing a modified binary grey wolf optimization and particle swarm optimization," *Expert Syst. Appl.*, vol. 204, Oct. 2022, Art. no. 117597.

[33] S. Ma, Y. Fang, X. Zhao, and Z. Liu, "Multi-swarm improved grey wolf optimizer with double adaptive weights and dimension learning for global optimization problems," *Math. Comput. Simul.*, vol. 205, pp. 619–641, Mar. 2023.

[34] X. Yu, W. Xu, and C. Li, "Opposition-based learning grey wolf optimizer for global optimization," *Knowl.-Based Syst.*, vol. 226, Aug. 2021, Art. no. 107139.

[35] S. Singh and J. C. Bansal, "Mutation-driven grey wolf optimizer with modified search mechanism," *Expert Syst. Appl.*, vol. 194, May 2022, Art. no. 116450.

[36] I. S. Millah, P. C. Chang, D. F. Teshome, R. K. Subroto, K. L. Lian, and J.-F. Lin, "An enhanced grey wolf optimization algorithm for photovoltaic maximum power point tracking control under partial shading conditions," *IEEE Open J. Ind. Electron. Soc.*, vol. 3, pp. 392–408, 2022.

[37] A. K. V. K. Reddy and K. V. L. Narayana, "Symbiotic learning grey wolf optimizer for engineering and power flow optimization problems," *IEEE Access*, vol. 10, pp. 95229–95280, 2022.

[38] Y. Yuan, X. Mu, X. Shao, J. Ren, Y. Zhao, and Z. Wang, "Optimization of an auto drum fashioned brake using the elite opposition-based learning and chaotic *k*-best gravitational search strategy based grey wolf optimizer algorithm," *Appl. Soft Comput.*, vol. 123, Jul. 2022, Art. no. 108947.

[39] W. Long, J. Jiao, X. Liang, S. Cai, and M. Xu, "A random opposition-based learning grey wolf optimizer," *IEEE Access*, vol. 7, pp. 113810–113825, 2019.

[40] W. Lei, W. Jiawei, and M. Zezhou, "Enhancing grey wolf optimizer with levy flight for engineering applications," *IEEE Access*, vol. 11, pp. 74865–74897, 2023.

[41] Q. Fan, H. Huang, Y. Li, Z. Han, Y. Hu, and D. Huang, "Beetle antenna strategy based grey wolf optimization," *Expert Syst. Appl.*, vol. 165, Mar. 2021, Art. no. 113882.

[42] W. Long, T. B. Wu, and M. Z. Tang, "Grey wolf optimization algorithm based on lens imaging learning strategy," *J. Automatic.*, vol. 46, no. 10, pp. 2148–2164, Oct. 2020.

[43] A. Achom, R. Das, and P. Pakray, "An improved fuzzy based GWO algorithm for predicting the potential host receptor of COVID-19 infection," *Comput. Biol. Med.*, vol. 151, Dec. 2022, Art. no. 106050.

[44] Y. Tian, J. Yu, and A. Zhao, "Predictive model of energy consumption for office building by using improved GWO-BP," *Energy Rep.*, vol. 6, pp. 620–627, Nov. 2020.

[45] K. Sowjanya and S. K. Injeti, "Investigation of butterfly optimization and gases Brownian motion optimization algorithms for optimal multilevel image thresholding," *Expert Syst. Appl.*, vol. 182, Nov. 2021, Art. no. 115286.

[46] M. Alazab, R. A. Khurma, and A. Awajan, "A new intrusion detection system based on moth-flame optimizer algorithm," *Expert Syst. Appl.*, vol. 210, no. 30, Dec. 2022, Art. no. 118439.

[47] H. H. Gul, E. Egrioglu, and E. Bas, "Statistical learning algorithms for dendritic neuron model artificial neural network based on sine cosine algorithm," *Inf. Sci.*, vol. 629, pp. 398–412, Jun. 2023.

[48] H. Liu, X. Zhang, H. Zhang, C. Li, and Z. Chen, "A reinforcement learning-based hybrid Aquila optimizer and improved arithmetic optimization algorithm for global optimization," *Expert Syst. Appl.*, vol. 224, Aug. 2023, Art. no. 119898.

[49] S. B. Aydemir, "Enhanced marine predator algorithm for global optimization and engineering design problems," *Adv. Eng. Softw.*, vol. 184, Oct. 2023, Art. no. 103517.

[50] M. Liu, X. Fu, L. Meng, X. Du, X. Zhang, and Y. Zhang, "Prediction of CO_2 storage performance in reservoirs based on optimized neural networks," *Geoenergy Sci. Eng.*, vol. 222, Mar. 2023, Art. no. 211428.

[51] Z.-B. Li, X.-Y. Feng, L. Wang, and Y.-C. Xie, "DC–DC circuit fault diagnosis based on GWO optimization of 1DCNN-GRU network hyperparameters," *Energy Rep.*, vol. 9, pp. 536–548, Apr. 2023.

[52] Q. Wang, C. Sun, and Y. Gu, "Research on SOC estimation method of hybrid electric vehicles battery based on the grey wolf optimized particle filter," *Comput. Electr. Eng.*, vol. 110, Sep. 2023, Art. no. 108907.

[53] K. Roushangar, S. Shahnazi, and H. M. Azamathulla, "Partitioning strategy for investigating the prediction capability of bed load transport under varied hydraulic conditions: Application of robust GWO-kernel-based ELM approach," *Flow Meas. Instrum.*, vol. 84, Apr. 2022, Art. no. 102136.

HAOJIE ZHANG is currently pursuing the Ph.D. degree with the College of Mechanical Engineering, Zhejiang University of Technology. His current research interests include laser-intelligent manufacturing and laser-intelligent integrated equipment technology

JIAXING CHEN is currently pursuing the master's degree with the College of Mechanical Engineering, Zhejiang University of Technology. His current research interests include laser-intelligent manufacturing and laser-intelligent process systems.

QUNLI ZHANG received the Ph.D. degree from the Zhejiang University. She is currently the Vice-President of the Institute of Laser Advanced Manufacturing, Zhejiang University of Technology, and a Ph.D supervisor. In the past few years, she has published more than 50 SCI and EI-indexed articles in the field of laser manufacturing. Her current research interests include laser surface engineering and laser intelligent manufacturing.

ZHIJUN CHEN received the Ph.D. degree from the Zhejiang University of Technology. He is currently an Associate Professor with the Institute of Laser Advanced Manufacturing, Zhejiang University of Technology. His current research interests include laser intelligent manufacturing equipment and laser manufacturing equipment integration technology.

XIAOYU DING received the Ph.D. degree from the Hefei University of Technology. He is currently an Associate Researcher with the Institute of Laser Advanced Manufacturing, Zhejiang University of Technology. His current research interest includes laser manufacturing technology.

JIANHUA YAO received the Ph.D. degree from Zhejiang University of Technology. He is currently the Dean of the College of Mechanical Engineering, the Director of the Institute of Laser Advanced Manufacturing, Zhejiang University of Technology, and a Doctoral Supervisor. He has published more than 300 SCI/EI-indexed articles. His research results have been widely applied in the manufacture of core components in high-end equipment fields, such as aerospace and power equipment, making important contributions to the technological upgrading of the equipment manufacturing industry. His current research interests include laser intelligent manufacturing and laser advanced manufacturing technology and equipment. He won the Second Prize in National Science and Technology Progress.